International Journal of Biological Macromolecules 281 (2024) 136500

Contents lists available at ScienceDirect

International Journal of Biological Macromolecules

journal homepage: www.elsevier.com/locate/ijbiomac

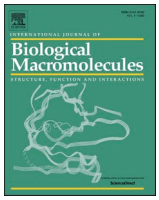

Neuropeptides regulate shell growth in the Mediterranean mussel (*Mytilus galloprovincialis*)

Zhi Li [a], Maoxiao Peng [a], Rute C. Félix [a], João C.R. Cardoso [a,*], Deborah M. Power [a,b,c,**]

[a] Comparative Endocrinology and Integrative Biology, Centre of Marine Sciences, Universidade do Algarve, Campus de Gambelas, 8005-139 Faro, Portugal
[b] International Research Center for Marine Biosciences, Ministry of Science and Technology, Shanghai Ocean University, Shanghai, China
[c] Key Laboratory of Exploration and Utilization of Aquatic Genetic Resources, Ministry of Education, Shanghai Ocean University, Shanghai, China

ARTICLE INFO

Keywords:
Bivalves
Mantle innervation
Neuropeptidome

ABSTRACT

In bivalves, which are molluscs enclosed in a biomineralized shell, a diversity of neuropeptide precursors has been described but their involvement in shell growth has been largely neglected. Here, using a symmetric marine bivalve, the Mediterranean mussel (*Mytilus galloprovincialis*), we uncover a role for the neuroendocrine system and neuropeptides in shell production. We demonstrate that the mantle is rich in neuropeptide precursors and that a complex network of neuropeptide-secreting fibres innervates the mantle edge a region highly involved in shell growth. We show that shell damage and shell repair significantly modify neuropeptide gene expression in the mantle edge and the nervous ganglia (cerebropleural ganglia, CPG). When the CPG nerve commissure was severed, shell production was impaired after shell damage, and modified neuropeptide gene expression, the spatial organization of nerve fibres in the ganglia and mantle and biomineralization enzyme activity in the mantle edge. Injection of CALCIa and CALCIIa peptides rescued the impaired shell repair phenotype providing further support for their role in biomineralization. We propose that the regulatory mechanisms identified are likely to be conserved across bivalves and other shelled molluscs since they all share a similar nervous system, a common mantle biomineralization toolbox, and shell structure.

1. Introduction

The Molluscs are one of the most diverse groups of soft-bodied invertebrate animals and the second most specious phyla after the insects [1–4]. They belong to the lophotrochozoans and are found in nearly all ecosystems on Earth playing a vital role in the maintenance of the structure and function of many ecosystems and as a source of food for humans and other taxa. The Mollusca phyla is composed of two major subclades, Aculifera (shell-less molluscs) and Conchifera (shell-bearing molluscs), which diversified ~546 million years ago (MYA) [5]. The Conchifera molluscs (Bivalvia, Cephalopoda, Gastropoda, Monoplacophora, and Scaphopoda), are the most diverse subclade and are proposed to have diversified ~540 MYA, and their calcified uni- or bivalved shells are equated with their evolutionary success and widespread distribution [4,6]. The evolution of molecules that regulate the rate of shell formation such as chitin was proposed to be a crucial step in Conchifera diversification [7–9]. Surprisingly little attention has been paid to the contribution of regulatory molecules and processes to mollusc evolution.

The vast diversity of forms, lifestyles and ecological niches of the Mollusca is matched by the high diversity and plasticity of their nervous systems including a centralized brain in cephalopods through to scattered ganglia in bivalves [10,11]. Studies of the giant squid axon generated seminal insights into nerve cell excitability [12,13] and gastropod slugs and snails continue to be important models for neurobiology [14]. Other Mollusca are less well studied although the basic architecture of the nervous system in most classes has been characterized [15–17]. The bivalves are the experimental model of the present study, and have a bilaterally symmetrical, decentralized, nervous system. In bivalves, three bilateral pairs of interconnected ganglia, the cerebropleural ganglia (CPG), visceral ganglia (VG) and pedal ganglia (PG) innervate and regulate the organism [18]. The CPG in bivalves is similar to the pleural ganglia of gastropods and innervates some of the same anatomical structures including the adductor muscle and visceral

* Corresponding author.
** Correspondence to: D.M. Power, J.C.R. Cardoso, Comparative Endocrinology and Integratie Biology, Centre of Marine Sciences, Universidade do Algarve, Campus de Gambelas, 8005-139 Faro, Portugal.
E-mail addresses: jccardo@ualg.pt (J.C.R. Cardoso), dpower@ualg.pt (D.M. Power).

https://doi.org/10.1016/j.ijbiomac.2024.136500
Received 19 June 2024; Received in revised form 29 September 2024; Accepted 9 October 2024
Available online 15 October 2024

nerve loop. The CPG in bivalves also innervates the anterior mantle, the labial tentacles, the mouth, and the oesophagus *via* the anterior pallial nerves [6]. The large paired VGs innervate many of the internal organs including the gills, heart, pericardium, kidneys, digestive tract, gonads, posterior mantle, and the sensory organs of the mantle, siphon, and cerebral mantle cortex [6]. In the scallops, the paired VGs are completely fused, forming a rudimentary 'brain' [18,19]. The PG nerves in the scallop innervate the foot as well as the anterior and posterior muscle tissues [6]. In the oyster, the PG is reduced in dimension, and this has been associated with the loss of the foot after metamorphosis. Available transcriptomes and proteomes of the ganglia in a) the bivalves, the Yesso scallop (*Patinopecten yessoensi*) and oysters (*Magallana gigas* and *Pinctata fucata*), b) the gastropods, the grey garden slug (*Deroceras reticulatum*), giant triton snail (*Charonia tritonis*), freshwater snail (*Biomphalaria glabrata*) and land snail (*Theba pisana*) and c) the cephalopod (*Sepia officinalis*) reveals the ganglia and neurons express a broad spectrum of proteins and neuropeptides.

Studies of a handful of neuropeptides identified before the advent of high throughput gene/protein sequencing assigned their functions mainly to growth, reproduction, and metabolism [20]. The first neuropeptide to be sequenced was isolated from the salivary glands of the octopus *Eledone muschata* [21]. Since then, a large neuropeptide repertoire has been identified in molluscs using omics and reveals relatively good conservation with the repertoire in Arthropods and Vertebrates [22], but the function of only a few have been characterized [23]. For example, in the Sydney Rock oyster (*Saccostrea glomerata*), the neuropeptides CCAP and APGW-amide are proposed to regulate reproduction [24] and in the gastropod, *Lymnaea stagnalis*, NPF/NPY neuropeptides are proposed to be involved in energy balance [25]. The FMRF-amide-like peptides in Mollusca are suggested to regulate the cardiovascular system, osmoregulation, reproduction, digestion, and feeding behaviour [26]. In the gastropods, the land snail (*Otala lacteal*) and the planorbid snail (*Helisoma duryi*), and a bivalve, the Pacific oyster (*M. gigas*), insulin-like peptides (ILP) are proposed to regulate mantle edge cell growth and shell growth [27–29].

The intriguing observation that neuropeptides can modulate shell growth in the Pacific oyster is supported by reports in other molluscs. For example, in the freshwater air-breathing snail *Helisoma*, shell damage modified the appearance of neurosecretory cells in the VG [30] and neurosecretory activity by the snail brain was associated with shell growth [31]. In the pond snail *L. stagnalis* two groups of neurosecretory light green cells (LGC) in the CPG secreted a hormone that stimulated shell and soft tissue growth and was later proposed to be an ILP [32,33]. Furthermore, in the ganglia of the slug, *Agriolimax reticulatus*, the neuropeptide somatostatin was proposed to regulate the growth of the periostaculum, which is a thin organic layer covering the shell in shelled molluscs [34].

The importance of the bivalve shell for survival means considerable attention has been focussed on shell construction, which occurs in the extrapallial space (EPS) a narrow-sealed cavity between the shell and mantle [35–37]. The mantle epithelial cells secrete chitin, and shell matrix proteins and provide a scaffold where Ca^{2+} and carbonate (CO_3^{2-}) ions secreted from the ciliated mantle and haemocytes can nucleate and crystalise to create the hard mineralized shell [36–40]. To improve understanding of shell production mantle transcriptomes and proteomes from bivalve species have been produced [41–43] and a biomineralization toolbox composed of matrix proteins, enzymes, ion channels, and species-specific genes has been proposed [44]. However, the role of regulatory factors on shell growth, and how they influence "shell toolbox" genes, and the response to environmental change is unknown. Recently long noncoding RNA were identified as a class of regulatory factors determining shell growth [45].

In our previous bivalve mantle transcriptome studies, we identified neuropeptides and their putative G protein-coupled receptors (GPCRs) and suggested they may be regulators of mantle function [46–48]. In addition, orthologues of the vertebrate calcitonin (CALC) system involved in calcium homeostasis, were identified in the mantle of *Mytilus galloprovincialis* [46] and *M. gigas* [49], and a role in calcium mobilization for shell production was proposed. Nonetheless, how CALC and other neuropeptides of the mantle interact to regulate shell growth has not yet been established and if neuropeptides of the bivalve nervous system have a function remains to be established. In this study, we explore the role of neuropeptides in shell growth and test the hypothesis that they do this by modulating the mantle's function. In a symmetrical bivalve, the Mediterranean mussel, *M. galloprovincialis* we a) explore and characterize the mantle neuropeptidome and compare it to other bivalves, b) look at the distribution of neurosecretory and neuropeptide fibres between the mantle and nerve ganglia, and c) conduct functional characterization of candidate neuropeptide genes to assess if they modify shell production by the mantle.

2. Material and methods

2.1. Animals and sampling

Mediterranean mussels (*M. galloprovincialis*) were collected from the Ria Formosa (Faro, Portugal, 37°00′32″N, 7°59′40″W) under the ICNF license 327 / 2022 / CAPT. Adult mussels (5.05 ± 0.32 cm long, 8.31 ± 1.34 g wet weight) were transported live to the Aquatic Organisms Experimental Laboratory at the Centre for Marine Science (CCMAR) where they were manually cleaned. Animals were acclimated for at least one week to the experimental system composed of 5-litre (l) glass aquarium filled with 4 l of aerated seawater (37 ppt, pH = 8.1 ± 0.1) from the bivalve's natural environment at ambient temperature (20–22 °C). During the acclimation period and experimental trials, mussels were fed daily (0.002 g / g body weight) with a mixture of a commercial dry microalgal (PHYTOBLOOM, Necton, Portugal). No mortality occurred during the acclimation or experimental period.

For tissue sampling, animals were placed on ice and the adductor muscle was severed with a sterile blade to allow the two valves to open. Samples from the mantle edge in the region most distal from the umbo (from here on designated as, the mantle) and CPG ganglia from control and experimental animals were collected, snap-frozen in dry ice, and stored at −80 °C until analysis. Mantle samples from control adult mussels were also collected and stored at −80 °C for transcriptome analysis and fixed overnight in 4 % paraformaldehyde at 4 °C for immunohistochemistry.

2.2. Shell regeneration experiments

Two holes next to each other (distance ~1 cm) were manually drilled (~ 2–3 mm in diameter) in the posterior edge of the shell of *M. galloprovincialis* without damaging the mantle. Three experimental challenges were performed (Supplementary Fig. 1).

2.2.1. Experiment 1. Determination of the timeline for shell regeneration after damage

The results of the first experiment were used to plan the subsequent experimental trials. Six animals ($n = 6$) were used, and shell regeneration was monitored at 1-, 5-, 9- 12-, 16- and 20-days post-damage by taking digital images of the damaged region in live animals to calculate the percentage of shell repair across time. The repaired area in each drilled hole/individual was calculated using the program ImageJ version 1.52a and the percentage of shell growth for each animal was taken as the average of the shell regrowth area in the two holes and calculated according to the formula: % hole area = (shell growth area/total hole area) × 100 %.

Because the mantle is involved in shell formation, we also aimed to characterize mantle mobility during the shell repair process the same experiment was repeated and the inner side of the valve was observed at 1-, 5-, 9-, 12-, 16- and 20-days post-damage. Animals were placed on ice and then the two valves were separated by carefully cutting the adductor

muscle with a blade. Digital photographs of the mantle attached to the inner side of the left valve of the damaged shell were taken. To confirm the presence of newly grown shell (covering the hole) and to detect any changes related to the shell repair process in the inner shell surface, the mantle was gently detached from the shell and digital images were taken (Supplementary Fig. 1B).

2.2.2. Experiment 2. Identification of candidate neuropeptide transcripts associated with shell regeneration

In this experiment the expression of candidate neuropeptide genes (Supplementary Fig. 1C) was determined in mantle tissue collected immediately below the drilled holes ($n = 6$ samples/group) and in the CPG ganglia ($n = 3$ samples/group, and each sample contained the CPG from 2 individuals) from control (non-drilled) and shell drilled (SD) animals at 12-, 24- and 36-hours post damage (SD-group).

Ten neuropeptide transcripts were selected for in-depth analysis based on the following criteria: a) expression and possible function in the mantle, as indicated by existing literature, b) the diversity of encoded mature peptides in the precursor genes, c) previously reported neuroregulatory activity in Mollusca and/or other invertebrates, d) the identification of a potential cognate receptor in the mantle transcriptome, and e) unknown mature peptide function.

The selected neuropeptide precursor candidates were: 1) the two calcitonin-like peptide precursors (CALCI and CALCII), previously suggested to have a role in the regulation of calcium movements across the mantle [46]. 2) The AST-C precursor proposed as a candidate immune factor in the mantle [47]. 3) Four members of the RF-amide family, a large, functionally diverse family of peptides in Mollusca [26,50], including i) the FxRI-amide peptide precursor that encodes 12 mature peptides and plays an important role as a neurotransmitter and neuromodulator in invertebrates [51], ii) LFRF-amide peptide precursor which encodes 6 matures peptides and has inhibitory activity in Mollusca neurons [26], iii) the CCK/SK peptide precursor for which a putative receptor was found in the mantle transcriptome (data not shown) and iv) the LFRY-amide peptide precursor a new member of the RF-amide family for which no function has been assigned. 4) The Mollusca Myomodulin precursor which encodes 10 putative mature peptides and is involved in the regulation of reproduction [52,53]. 5) The Lophotrochozoan APGW-amide peptide precursor which encodes 9 mature peptides and regulates reproduction in gastropods [54] and 6) the LRNFV-amide peptide precursor which encodes 11 peptides with no known function.

2.2.3. Experiment 3. The role of the nerve ganglia in shell regeneration

To identify which nerve ganglia was involved in shell repair, a preliminary experiment was conducted. The commissure between the paired CPG (CPG-group) and between the paired VG (VG-group) ganglia was cut (Supplementary Fig. 1D). This was done by placing animals on ice, and slightly opening their shells with a clam shell opener. Using a fine needle, the body tissues were gently separated to expose the ganglia. The CPG and VG commissures were cut using fine scissors. Then two holes were drilled in each valve as previously described, and the animals were immediately placed in seawater. The CPG and VG were targeted because, a) both CPG and VG are proposed to innervate the mantle edge and control mantle movement [55], b) neuropeptide precursors have previously been identified in both ganglia in other bivalve transcriptome studies [23,56], and c) the CPG and VG ganglia are easy to access and manipulate. Each group (control, CPG-group and VG-group) contained 8 animals and the repair rate of the holes in the left and right valves of the CPG-sectioned group was monitored and measured at 0, 5 and 10 days after drilling, while for the VG-sectioned group it was monitored at days 0 and 7. To understand the impact of ganglia damage on mantle movement the third shell repair experiment was repeated and the mantle on the inner side of the left valve was observed at 2, 5, 9 and 20 days after the damage and photographed as described above. Additionally, a group in which both CPG and VG commissures were severed (CPG + VG-group) was established, and shell repair and mantle movement were monitored. No mortality was observed in any of the experimental groups during the experiment.

After examining the regrowth of shells when the ganglia were severed, it was determined that damage to the CPG -ganglia commissure had the most significant inhibitory effect on shell repair. To further investigate the relationship between the CPG and the mantle, another experiment was conducted. Adult mussels ($n = 48$ total) were randomly assigned to three groups ($n = 16$ per group): 1) intact control animals (C), 2) shell-damaged group (SD-group) with an intact nervous system, and 3) a group with shell damage and a severed commissure between the CPG ganglia (CPG-group). On day 0, the mantle tissue beneath the drilled holes was collected from the SD-group and CPG-group ($n = 8$ mussels/ group) and from the C group (n = 8 mussels). The trial duration was determined based on the results of experiment one. At day 0 and at the end of the 10th day the mantle (located below the drilled shell or its equivalent position in the control group) was collected from all experimental groups for analysis of changes in gene transcript expression.

All the experimental trials were carried out during October–December 2022 under natural photoperiod (winter in the Algarve) and at ambient room temperature (20–22 °C). Half of the water in each aquarium was renewed every two days and the aquaria were manually cleaned. The regenerating shell in each drilled hole was inspected at each sampling timepoint under a stereoscope (Motic, SMZ-171, China) equipped with a digital camera (Visicam 6 Plus, VWR, Portugal). Digital images of the shells were taken from the mussels of experiment 1 ($n = 6$ animals/ time point) at 0, 1-, 5-, 9-, 12-, 15- and 20-days post-drilling and from experiment 3 on day 0, 5 and day 10 ($n = 8$ animals/ time point) and the repaired area in each drilled hole/individual was calculated using the program ImageJ version 1.52a. The percentage of shell growth in each animal was calculated by averaging the shell regrowth area in the two holes and using the formula: % hole area = (shell growth area/ total hole area) × 100 %.

2.3. Total RNA extraction and cDNA synthesis

Total RNA was extracted using an ENZA kit (VWR, USA) and any contaminating genomic DNA was removed by treating with Precision DNase as recommended by the manufacturer (Primer design, UK). For total RNA extraction, the collected tissue composed of the mantle and CPG ganglia with the commissure nerves from control and experimental animals were thawed on ice in lysis buffer and then mechanically disrupted using a Tissue lyser II (Qiagen, Germany) with two iron beads (5 mm) for 3 min at room temperature. The concentration and quality of the extracted total RNA were assessed by determining their absorbance using a NanoDrop (Thermo Scientific, USA) and by agarose gel (1 %) electrophoresis.

For cDNA synthesis, DNase-treated total RNA (500 ng) was denatured at 65 °C for 5 min and quenched on ice for 5 min. The reactions for cDNA synthesis were carried out in a final reaction volume of 20 μl and contained 10 ng of pd. (N) 6 random hexamers (Jena Bioscience, Germany), 2 mM dNTPs (ThermoScientific, USA), 100 U of RevertAid Reverse Transcriptase and 8 U Ribolock RNAse inhibitor (ThermoScientific). Reaction conditions were as follows: 10 min at 20 °C; 60 min at 42 °C and finally 5 min at 70 °C. The quality and uniformity of the synthesised cDNA for all samples were assessed by amplification of the mussel 18S ribosomal subunit (18S rRNA) using specific primers (Table 1) and the following thermocycle: 95 °C, 3 min; 25 cycles (95 °C, 20 s; 60 °C, 20 s; 72 °C, 20 s); 72 °C, 5 min. The reaction products were assessed by agarose gel (2 %) electrophoresis.

2.4. Mantle transcriptomes and analysis

The mantle from the left and right valve of control adult *M. galloprovincialis* ($n = 6$ / shell side) was collected and total RNA was extracted using an ENZA kit (VWR, USA) as described above. Library

Table 1
List of primers used in qRT-PCR analysis for the bivalve *M. galloprovincialis*.

Transcript		Sequence (5′ à3′)	T (°C)	Efficiency	R^2
CALCI	Fwd	TGGTTGAAACTTACATGTGGTT	60 °C	95.40 %	0.997
	Rev	CATTCTTCTTCAATGACGTCA			
CALCII	Fwd	AAACGGGCGTGCAATCTTG	58 °C	94.70 %	0.997
	Rev	CGAATGTTCTTTAGGTCAAGGC			
CCK/SK	Fwd	CCGGTGCGATATTTCTGTAGG	60 °C	87.30 %	0.996
	Rev	ACACATTGTGCACTTACCGT			
LFRY-amide	Fwd	TAGAATTATGTGCTGAAGGGA	60 °C	87 %	0.997
	Rev	ATATTGCTGTAATCCTGAAGGA			
APGW-amide	Fwd	CATCTTCAGATGAGTCGAGTG	58 °C	81.10 %	0.999
	Rev	CTTCGGAATCGAACAACATATC			
Myomodulin	Fwd	ATTAACCCAGGACCTCGTCC	58 °C	79.20 %	0.997
	Rev	TCTTCTGTGAGGTATCTACC			
LFRF-amide	Fwd	TTGGACACCAGGACGATAAC	60 °C	96.50 %	0.991
	Rev	CTAATTCCTCCTCACGACCA			
FxRI-amide	Fwd	CAAGATGGGACCTGAATATG	58 °C	94.70 %	0.999
	Rev	GATTTAACTCAGCACTCCTC			
ASTC	Fwd	GCAGTTTCAAGAGCAGGAAGCCT	66 °C	96.80 %	0.997
	Rev	GGCATTGCACATGGCTTCGTTT			
LRNFV-amide	Fwd	TGCGTACACTATCTTCTGGT	58 °C	92.80 %	0.999
	Rev	AATTCAAACCACGGAAGCAC			
18S	Fwd	GTGCTAGGGATTGGGGCTTG	60 °C	95.50 %	0.999
	Rev	TAGTAACGACGGGCGGTGTG			
EF1 α	Fwd	GAAGGCTGAGGGTGAACGTG	60 °C	96.20 %	0.996
	Rev	TCCTGGGGCATCAATAATGG			

preparation and sequencing were performed by Novogene Europe. Before library production, the total RNA integrity of the samples was assessed using an RNA Nano 6000 Assay Kit for a Bioanalyzer 2100 system (Agilent Technologies, CA, USA) and only samples that passed a pre-established threshold for the RNA integrity (RIN $>$ 8.0) were used for library preparation ($n = 3$ samples /shell side and each sample was composed of a pool of total RNA from two individuals). Sequencing was performed with an Illumina NovaSeq 6000 and 150 base paired-end reads were generated.

Mantle transcriptomes were analysed in Galaxy (https://usegalaxy.eu/) and annotated in R-studio. The quality of the transcriptome was assessed using FastQC (Version 0.72) with the default parameters [57] and Trimmomatic (Version 0.36.5) was used to trim low-quality reads [58]. Clean reads from the two mantle valves were combined and mapped to the annotated reference genome of *M. galloprovincialis* (NCBI Accession: GCA_900618805.1) in GenBank using HISAT2 (Version 2.1.0, default settings) and transcript counts generated with StringTie (Version 1.3.6, default settings). Sequences were deposited in SRA with the project PRJNA995578 in N°. SAMN36494222. The mantle transcriptomes were generated in the context of another project, which provides in-depth analysis of the data [59]. In the present study, the transcriptomes were exclusively used to identify putative neuropeptide-encoding genes, which were not the focus of the other study.

2.5. Sequence database searches and annotations

The presence of putative neuropeptide precursor genes in the predicted proteins of the *M. galloprovincialis* genome at NCBI (GCA_900618805.1) was established by searching the database using as the query the deduced neuropeptide precursor orthologues from the Pacific oyster (*C. gigas*, now renamed *M. gigas*) and the scallop (*M. yessoensis*) [23,60,61]. A total of 110 bivalve neuropeptide precursor genes (Supplementary Table 1), 60 from *M. gigas* and 50 from *M. yessoensis* were used to search the predicted proteins of *M. galloprovincialis* (taxid:29158) using the blastp programme and hits with an e value < -10 were retrieved and analysed. To identify candidate neuropeptide genes with the potential to regulate mantle function, *M. galloprovincialis* mantle transcriptome reads were mapped to the annotated genome. Only genes identified in more than one of the mantle transcriptome libraries generated for the right or left valve ($n = 3$/ each valve) were included in subsequent analysis. Additionally, assembled, and annotated *M. galloprovincialis* mantle transcriptomes (SRP 063654) available "in-house" [41] were also searched for the neuropeptide sequences since the reference genome annotation (NCBI, GCA_900618805.1) available for *M. galloprovincialis* is incomplete [62].

The identity of the retrieved *M. galloprovincialis* putative neuropeptide coding genes was confirmed by characterization of the deduced protein precursors and localization of the predicted mature peptides by a) the identification in the flanking sequences of monobasic, dibasic, or tribasic consensus cleavage sites (RR, KR, KK) and b) identification of conserved mature peptide motifs [23,60]. The *M. galloprovincialis* peptide precursors were aligned with the orthologues from *M. gigas* and *M. yessoensis* using the multiple sequence alignment programme clustal omega with the default settings [63] to confirm sequence homologies and the deduced mature peptides were annotated.

2.6. Tissue histology and immunofluorescence

The mantle edge was collected and fixed overnight (16 h) with gentle agitation in 4 % paraformaldehyde (PFA) at 4 °C. Tissue was rinsed in water and dehydrated through a graded ethanol series (70 % to 100 %), saturated in xylene and embedded in paraffin wax (Merck, Germany). Serial transverse sections (5 μm) were mounted on glass slides and dried overnight at 37 °C, cooled to room temperature and stained using a standard hematoxylin and eosin (H&E) procedure to characterize the general morphology of the mantle using a microscope (Leica DM2000) connected to a digital camera (Leica DFC480).

Immunofluorescence was performed to a) characterize the neuropeptide secretory fibres in the mantle and b) analyse the organization of the nerve fibres in the ganglia (CPG and VG) and mantle during shell repair and after severing the CPG commissure in mussels. Mantle, CPG ganglion and VG ganglion tissue samples were equilibrated with a graded series of sucrose solutions (from 10 % to 30 %) and stored at −20 °C until use. To prepare the tissue for sectioning, they were embedded in an optimal cutting temperature (OCT, VWR, Portugal) medium and frozen at −20 °C overnight. Serial sections of 14 μm were prepared using a cryostat (NX50 cryostat, Thermo Scientific, Waltham, MA, USA) and mounted on glass slides (treated with APES; Sigma-Aldrich, Madrid, Spain) before being stored at −20 °C.

For immunofluorescence, slides were washed 3 times in PBS for 15 min and then incubated in OCT blocking solution (Tris-Carrageenan-Triton X buffer, 0.1 M Tris buffer containing 0.7 % Carrageenan and 0.5

% Triton X-100, pH 7.6) containing 3 % sheep serum (Sigma-Aldrich, Madrid, Spain) for 2 h at 4 °C. The primary antisera utilized were anti-FMRF (rabbit polyclonal, Immunostar, 20091) diluted 1:1000 in PBS, anti-β-tubulin (mouse monoclonal, Sigma, T-4026) diluted 1:250 in PBS and anti-5-HT (rabbit polyclonal, Sigma, S-5545) diluted 1:400 in PBS (Table 2). The specificity of the primary antisera used in the study has previously been validated in other studies of invertebrates [64,65].

Mantle tissue sections were incubated with FMRF, serotonin and β-tubulin antisera and the CPG and VG sections were incubated with serotonin and β-tubulin antisera. For all tissue sections incubation with the primary antisera at the optimal dilution was overnight at 4 °C, rinsed twice in PBS for 5 min and then incubated with the secondary antisera in the dark and in all subsequent steps of the procedure. The secondary antisera were Alexa Fluor 546-conjugated anti-rabbit IgG (Molecular Probes, Eugen, Oregon; A-11035) for the FMRF and serotonin antisera, and Alexa Fluor 546-conjugated anti-mouse IgG (Molecular Probes, Eugen, Oregon; A-11030) for the β-tubulin antisera. The sections were incubated with the appropriate secondary antisera for 2 h at room temperature in the dark and then washed twice in PBS (3 min per wash) and the nuclei stained with a solution of DAPI (1:20000 dilution, Sigma, St. Louis, MO, USA) for 5 min. After two washes of 3 min in PBS, tissue sections were mounted in glycerol-gelatine (Sigma-Aldrich, GG1, Madrid, Spain) and analysed using a fluorescence microscope (Zeiss Axioimager Z2, Carl Zeiss Group) coupled to a digital camera (Axiocam ICC3) linked to a computer for digital image analysis.

2.7. Quantitative PCR

Changes in neuropeptide gene expression during shell repair were assessed in the RNA extracted from mantle tissue below the drilled area and in the CPG-ganglia by quantitative real-time PCR (qPCR) using SsoFast EvaGreen Supermix (BIO-RAD, Portugal). A 5 μl final reaction volume was prepared with 200 nM of forward and reverse gene-specific primers (Table 1**)** and 1 μl of template cDNA (diluted 1:3). The expression of elongation factor 1-alpha (*ef1α*) and 18S ribosomal subunit (*18 s*) transcripts in *M. galloprovincialis* cDNA (diluted 1:50 and 1:500, respectively) did not vary between samples and so they were used as reference genes. Duplicate reactions were performed (< 5 % variation between replicates) using a CFX Connect Real-Time PCR Detection System for 384-well microplates (BIO-RAD). Cycling conditions were 95 °C, 30 s; 44 cycles (95 °C for 5 s and 10 s at the primer annealing temperature, Table 1). To detect non-specific products and primer dimers melting curves were performed. q-PCR efficiencies and R^2 (coefficient of determination) were established (Table 1) and gene expression levels were calculated. Data was normalized using the geometric mean of the reference genes. All amplicons were sequenced to confirm reaction specificity.

Table 2
List of the primary and secondary antibodies used for the immunohistochemistry.

Antibody	Host species	Source	Dilution before use
FMRF_amide	Rabbit (polyclonal)	Immunostar (20091)	1:1000
β-tubulin	Mouse (monoclonal)	Sigma (T-4026)	1:250
Serotonin (5-HT)	Rabbit (polyclonal)	Sigma (S-5545)	1:400
Alexa Fluor 546-anti-rabbit IgG	Donkey	Molecular Probes, Eugen (A-11035)	1:400
Alexa Fluor 546-anti-mouse IgG	Donkey	Molecular Probes, Eugen (A-11030)	1:400

2.8. Enzymatic assays

The effect of the experimental manipulations on the activity of mantle carbonic anhydrase activity the enzyme that generates bicarbonate from metabolic carbon dioxide and so regulates the formation of the mineralized calcium carbonate crystals in the shell was determined [46,66,67].

2.8.1. Mantle protein extracts

Protein extracts were prepared from the mantle of both valves for the enzymatic assays. Mantle samples from the control (C), SD-group and CPG-group mussels at 0 and 10 days were used. Mantle protein extracts were prepared in sterile SW by mechanically disrupting the tissue using a Tissue lyser II (Qiagen, Germany) with two iron beads (5 mm) for 3 min at room temperature. The amount of SW added was 10 times the tissue weight to obtain a final concentration of 0.1 mg /μl of the protein extract. The lysate was centrifuged for 15 min at 13000 rpm and the supernatant was transferred to a clean tube and stored at −80 °C until use. Samples were used within 4 days of preparation.

2.8.2. Esterase activity

Esterase activity in the mantle (n = 8/ group) was quantified in protein extracts using a colorimetric assay that measured the conversion of the substrate 4-nitrophenyl acetate to p-nitrophenolate. Assays were performed using the method previously described [46,68]. In brief, 10 μl of mantle edge protein extracts (0.1 mg /μl) were added to 290 μl of the substrate (0.05 M 4-Nitrophenyl acetate (Acros Organics, USA) in Tris-HCl (pH 7.4) for 20 min in the dark with gentle agitation. Reactions were performed at RT in duplicate for each of the extracts prepared. Esterase activity was stopped by placing the reactions on ice for 5 min and the absorbance was read at 405 nm (Biotek Synergy 4, USA). The amount of p-nitrophenolate produced was quantified using a standard curve prepared from p-nitrophenol (from 0 to 200 μM). Bovine CA isoenzyme II (0.1 mg/ml) (Sigma-Aldrich) was used as the positive control.

2.8.3. Acid phosphatase activity

Acid phosphatase activity (n = 8/group) in mantle protein extracts was determined using 96 well-plates (Greiner, Germany) and a tartrate-resistant acid phosphatase (TRAP) assay as described in [46]. Briefly, 10 μl of the mantle edge protein extract (0.1 mg/μl) was added to 190 μl of TRAP buffer (20 mM para nitrophenyl (pNPP, Sigma-Aldrich), 20 mM tartrate in 0.1 M Na-acetate buffer, pH 5.3) and incubated for 20 min at RT with agitation. Reactions were stopped with 2 M NaOH and measured at 405 nm using a microplate reader (Biotek Synergy 4). The amount of pNPP converted into p-nitrophenol (pNP) was calculated using a pNP standard curve (from 0 to 200 μM) prepared as outlined above.

2.8.4. Alkaline phosphatase activity

Alkaline phosphatase (ALP) activity (n = 8/ group) in mantle protein extracts was determined using 96 well-plates (Greiner) according to the protocol described in [46]. Briefly, 10 μl of the mantle protein extract (0.1 mg/μl) was added to 190 μl of ALP buffer (5 mM para-nitrophenylphosphate – pNPP, Sigma-Aldrich –, 0.1 M Tris-HCl – pH 9.5–1 mM $MgCl_2$, and 0.1 mM ZnCl). For ALP reactions, the samples were incubated with agitation at 30 °C in the dark for 30 min. The reactions were stopped by adding 200 μl of 2 M NaOH and 150 μl of the reaction mix from each well was transferred in duplicate to a 96-well plate and absorbance was measured at 405 nm using a microplate reader (Biotek Synergy 4). The amount of pNPP converted into pNP was calculated using a pNP standard curve (from 0 to 200 μM) prepared as outlined above.

2.9. Peptide injections

To assess if the candidate peptides identified regulate shell formation, a shell damage-repair assay was carried out in bivalves. Several neuropeptides were selected as candidates for shell growth, based on the following criteria a) in shell damage-repair assays they had a significantly modified gene expression compared to the control individuals, and/or b) they had a significantly modified gene expression after the commissure of the CPG ganglia was severed (see Section 2.2 for experiments).

In *M. galloprovincialis* with two holes drilled in the right and left valve, candidate peptides were injected into the adductor muscle using a micro-syringe (Hamilton Gastight Syringes, Germany) with a 23G needle and their effect on mantle function and shell formation was assessed. Candidate peptides that were tested included CALCIIa (H-CTWGGGMSDEMCSTVDIDEIQRSFQVIHDRNSP-amide), which is encoded in the *M. galloprovincialis* CALCII precursor, a candidate regulatory factor of shell mineralization [46] and the MYOc peptide (AMPMLRL-amide, repeated 3 times inside the Myomodulin precursor). The peptide CALCIa (H-ACNLGLNSHHCALADLDNQLQS REWLSNGHSP-amide) was also tested because it is the duplicate of CALCIIa [46] and a further peptide CCK/SK (QGDWDLDYGLGGGRW-amide) was included as a negative control because its expression was unrelated to shell growth and the peptide was synthesised without the sulphate group, so it does not activate its receptor.

All the peptides were synthesised with a purity > 95 % by HPLC analysis. Modifications including N-terminal acetylation, C-terminal amidation and appropriate disulphide bonds were included for CALC peptides and for MYOc and CCK/SK the peptides were amidated (GL Biochem Ltd., Shanghai, China). All peptides were re-suspended in sterile 1× PBS before the assays. To choose the best concentration of peptide for the *in vivo* assays, optimization studies with three concentrations (10^{-4}, 10^{-5} and 10^{-6} M) were initially tested, by injecting (50 μl) of them into the adductor muscle and monitoring shell re-growth for 5 days. In the PBS group, PBS alone (50 μl) was administrated. A control group was included to represent the normal repair process (no manipulation). For the trial, a peptide concentration of 10^{-5} M was chosen. Only the peptides (CALCIa, CALCIIa and MYOc) that affected shell growth were tested. CCK/SK, which had no effect in the optimization trials, was excluded (Supplementary Fig. 2). Thirty *M. galloprovincialis* were randomly divided into 5 groups of 6 animals each and placed in 10 l tanks filled with seawater from their natural habitat. Peptides and PBS injections (50 μl) were administered every 48 h throughout the experimental.

Experiments were run under the conditions described above (Section 2.1) except that the temperature of the seawater was 25–27 °C and the photoperiod was that for August in the Algarve. No mortality was observed during the experiments. The regenerated shell inside the holes drilled in each valve was observed daily under a stereomicroscope and photographed using a digital camera (Visicam 6 Plus, VWR, Portugal). The shell repair rate was calculated on day-15 after the start of the experiments from six ($n = 6$) biological replicates per group and was the average of the two holes in the two valves (right and left) of each animal. This experiment was repeated independently twice.

2.10. Scanning electron microscopy (SEM)

Regenerated shells from *M. galloprovincialis* were washed with distilled water, air-dried, and used for SEM imaging. Shell samples were mounted on stubs coated with gold (JEOL, JFC1200, JSM Electron Microscopes, Tokyo, Japan), and observed using a scanning electron microscope (JEOL, JSM5200-LV, JSM Electron Microscopes, Tokyo, Japan) with a high-energy beam of 25 kV, and images were acquired after 90 s exposure using digital software.

2.11. Calcein staining and IR spectral analysis of regenerating shells

A section of the newly grown shell (~0,3 cm^2) of the control and shell rescue mussels injected with PBS (negative control) or with CALCIa, CALCIIa or MYOc peptides were collected 7 days post-damage and immersed for 16 h in a 100 mg/l calcein (Sigma-Aldrich) solution prepared with sterile filtered seawater. Shells were subsequently rinsed in 1xPBS, observed under a fluorescence microscope (Zeiss Axioimager Z2, Carl Zeiss Group) and digital images were captured using a digital camera (Axiocam ICC3). A small section of the regrown shell from each experimental group was also analysed using Attenuated Total Reflectance Fourier Transform Infrared (ATR-FTIR) spectroscopy (Thermo Scientific Nicolet iN10 MX, USA) and compared to the mineralized control shell. The FITR spectrum was taken with an aperture of 100 μm/100 μm, a range of 700–4000 cm^{-1} and a resolution of 8 cm^{-1}, and the accumulation of 64 scans. Data acquisition was performed using OMNIC Picta software and the $CaCO_3$ signal was identified by comparison with the reference spectrum [69–70]. A heat-map of the regenerated shell section in the control and experimental groups was constructed using the characteristic absorbance signal of $CaCO_3$ found at the wavelength, 1795.93 cm^{-1}.

2.12. Statistical analysis

Statistical analysis was performed using GraphPad Prism version 8.0 for Mac OS X (US, www.graphpad.com). One-Way ANOVA and Two-Way ANOVA with a Sidak's multiple comparisons test were used. All the results are shown as mean ± standard error of the mean (SEM). One-Way ANOVA was used to identify significant differences between experimental groups in the enzymatic assays and shell repair experiments. Two-Way ANOVA was utilized to determine significant differences in gene expression between groups and to assess the impact of the peptides on shell growth. The significance threshold was set at $p < 0.05$.

3. Results

3.1. Neuropeptide precursors in M. galloprovincialis

To explore the diversity of neuropeptide precursors found in the *M. galloprovincialis* genome and to identify those expressed in the mantle, the neuropeptide gene set was obtained from the genome and then their expression was determined in the mantle by analysing transcriptomes. Sequencing of the 6 mantle cDNA libraries ($n = 3$/ each shell side) of control adult mussels yielded an average number of reads of 43771022 per library with an average GC content of 38 %. They were combined and mapped against the *M. galloprovincialis* annotated genome and yielded a total of 83,135 genes. This suggests that approximately 62 % of the genes predicted in the *M. galloprovincialis* genome (a total of 134183 predicted genes) are expressed in the mantle [45].

Searches in the *M. galloprovincialis* annotated genome using full-length peptide precursors or deduced mature peptide sequences from other bivalves identified at least 48 neuropeptide gene family members that were orthologues of neuropeptide genes and precursors found in *M. gigas* and *M. yessoensis* (Fig. 1, Supplementary Table 1). To confirm genome predictions and identify additional neuropeptide families or family members that have not been identified in the available annotated genome, annotated mantle transcriptomes available "in house" were searched and 6 additional neuropeptide precursor transcripts (Allatostatin C, Allatotropin, CALC I, FF-amide, FxRI-amide and opioid) were identified [41,46,47].

In *M. galloprovincialis* most neuropeptide genes corresponded to a single protein precursor but for some multiple precursors were predicted (Fig. 1, Supplementary Fig. 3 and Supplementary Table 1). Two protein precursors were predicted for 16 neuropeptide gene families: Bursicon, Calcitonin (CALC), Conopressin, Feeding Circuit-Activating Peptide (FCAP), Insulin-like peptide (ILP), LASGLV_amide, Luqin, LRY-amide,

		Mga	Mgi	Mye	Mga	Mgi	Mye		
Bilaterian	Conopressin	2	1	1	2	2	2	Bursicon	
	GnRH	1	1	1	1	1	1	FMRF_a	
	CCK/SK	1	1	1	3	1	1	Elevenin	
	sCAP	2	1	1	1	2	1	Prohormone 4	
	NPF	3	1	1	1	1	1	GNQQNxP	
	DH44	1	1	1	1	1	1	**APGW_a**	Lophotrochozoan
	CALC	2	2	2	2	1	1	LASGLV_a	
	CCAP	1	1	1	1	1	1	**LFRF_a**	
	GGN_a	1	1	1	1	1	1	**LFRY_a**	
	GPA2/GPB5	1	1	1	1	1	1	**LRNFV_a**	
	ILP	2	2	3	1	1	1	MIP	
	Opioid	1	1	1	2	0	1	PFVx7_a	
	7B2	1	1	0	2	1	1	WX3Y_a	
	Buccalin	3	1	1	1	1	1	GWE_a	
	Prokineticin	5	4	0	1	1	1	**FxRI_a**	
	LRY_a	2	1	1	1	3	1	QS_a	
	Allatotropin	1	1	1	1	3	1	Achatin	Mollusca
	FF_a	1	1	1	2	1	2	FCAP	
	Urotensin	1	1	0	2	2	1	**Myomodulin**	
Protostome	Luqin	2	1	1	2	1	1	NKY	
	AST-B/MIP	2	1	1	1	3	2	Pedal peptide	
	PKYMDT	1	1	1	1	2	1	FYFY_a	
	Cerebrin/PDF	1	1	1	1	1	1	GN_a	
	AST_C	1	1	1	2	1	0	RxI_a	

Fig. 1. Minimum neuropeptidome in the *M. galloprovincialis* genome. Comparisons of the number of *M. galloprovincialis* (Mga) neuropeptide gene transcripts with *M. gigas* (Mgi) [60] [61] and *M. yessoensis* (Mye) [23]. The numbers inside the boxes represent the number of genes. The accession numbers of the predicted peptide precursors, length and number of mature peptides is available in Supplementary Table 1. The complete neuropeptide precursor sequences and deduced mature peptides for *M. galloprovincialis* are available in Supplementary Fig. 3 and the sequence alignment of the deduced mature peptides between Mga, Mgi and Mye are available in Supplementary Fig. 4. The peptide precursors found in the mantle transcriptomes are marked in blue and those selected for genes expression and functional analysis are in bold.

Allatostatin B/ Myoinhibiting peptides (AST-B/MIP), Myomodulin, neuropeptide KY (NKY), PFVx7, RxI_amide, small Cardioactive Peptide (sCAP) and WX3Y_amide peptide, three protein precursors were retrieved for Buccalin, Elevenin and neuropeptide F (NPF) and five for the Prokineticin neuropeptide gene (Fig. 1, Supplementary Tables 1 and 2). Most of the predicted protein precursors resulted from alternative exon splicing events of a single gene (Supplementary Table 2). However, in the case of Bursicon, CALC, ILP, PFVx7 and Prokineticin the predicted peptide precursors arose from different genes (Supplementary Table 2).

Precursors encoding neuropeptide genes that are conserved across bilaterians (19), Protostomes (5), Lophotrochozoans (16) and Mollusca (8) were identified (Fig. 1). Comparisons between the bivalve species *M. gigas*, *M. yessoensis* and *M. galloprovincialis* suggested that the number of neuropeptide precursors and encoded mature peptides was species-specific (Fig. 1, Supplementary Table 1, Supplementary Fig. 4). In *M. galloprovincialis* the largest and most peptide-rich neuropeptide precursor was the pedal peptide precursor and a single gene encoding the peptide precursor was found. The predicted peptide precursor encoded 23 mature peptides. In *M. gigas*, 3 different genes encoding the pedal precursors have been described and the predicted peptide precursors encoded a different number of mature peptides (27, 11 and 16 peptides) [60]. In *M. yessoensis* two gene orthologues encoding the pedal precursors were described and encoded 9 and 7 mature peptides [23] (Supplementary Table 1). Other examples of predicted peptide precursors encoding multiple peptides were the bivalve FMRF-amide precursors which encoded 16, 14 and 27 mature peptides in *M. galloprovincialis*, *M. gigas* and *M. yessoensis*, respectively (Fig. 1, Supplementary Table 1, Supplementary Fig. 4).

Interrogation of adult *M. galloprovincialis* mantle transcriptomes identified at least 45 neuropeptide transcripts that belonged to 41 different neuropeptide gene families (Supplementary Table 3). Of all the neuropeptide gene families identified only members of Bursicon, GWE-amide and Neuropeptide prohormone 4 gene families were not identified. Ten (10) neuropeptide precursors were selected for gene expression analysis and functional studies to explore their involvement in mantle-shell production and biomineralization (Fig. 1, Supplementary Fig. 3).

3.2. Detection of neuropeptide fibres in *M. galloprovincialis* mantle

H&E staining of tissue sections revealed the general tissue morphology and the three mantle folds were readily identified, and were composed of loose connective tissue bordered by columnar epithelial cells. We investigated the origin of neuropeptides in the mantle by studying the distribution of neuropeptide fibres and mapping the mantle fibres containing the neuropeptide FMRF. We used antisera commercially available, which were previously validated for use in molluscs [55] (Fig. 2). The mantle of *M. galloprovincialis* is made up of three distinct folds: the outer fold (OF), middle fold (MF), and inner fold (IF). FMRF immunopositive fibres were found in the inner mantle and in the mantle margin, indicating that this tissue is highly innervated, and contains a complex network of FMFR fibres. Additionally, concentrated nerve tracts of varying size were detected within the inner mantle tissue (Fig. 2). This confirmed that the mantle in *M. galloprovincialis* is highly innervated and suggested that it is regulated by the ganglia and indicates that neuropeptides such as FMRF may play an important role.

3.3. The impact of ganglia damage on shell regeneration

3.3.1. Implementation of an in vivo *M. galloprovincialis* shell regeneration model

To study the potential role of neuropeptides in mantle function, we examined their potential involvement in shell production. For this purpose, we established an experimental model to observe shell damage and repair in living bivalves. In our experiment, we drilled a hole in both shell valves and monitored the shell regeneration process. After 20 days the hole in the valve was fully repaired with new shell (Fig. 3A). Normal shell regeneration occurred at a variable rate across time (Fig. 3A) and the most intense period of repair occurred within the first days after the shell was drilled and by the 5th day more than half (64 ± 4 %) of the hole was covered by newly grown shell. The subsequent repair rate was slower, and it took a further 15 days (until day 20), for the drilled hole to be totally covered (Fig. 3A). Moreover, no differences were observed in the rate of shell regrowth when the left and right drilled valves were compared suggesting that shell regeneration occurred at a similar rate after damage in both valves (Fig. 4A).

Observations of the mantle movements during shell repair were carried out during the initial stages of shell repair. After drilling, the mantle edge retracted and surrounded the hole (Fig. 3B). After the shell was repaired, the mantle slowly returned to its original position before drilling. Twenty (20) days after drilling, when the hole was completely covered by a thin mineralized layer, the mantle was close to its original position before drilling as seen in Fig. 3B. During the shell repair process morphological changes were observed in the prismatic layer of the inner shell surface surrounding the anterior region of the drilled hole (Fig. 3C). Light microscopy revealed that an irregular matrix structure was formed during repair.

3.3.2. Severing the CPG in vivo impairs shell-regeneration in *M. galloprovincialis*

To assess the potential regulatory role of the nervous ganglia on shell repair/growth, the nerve commissure that connects the left and right

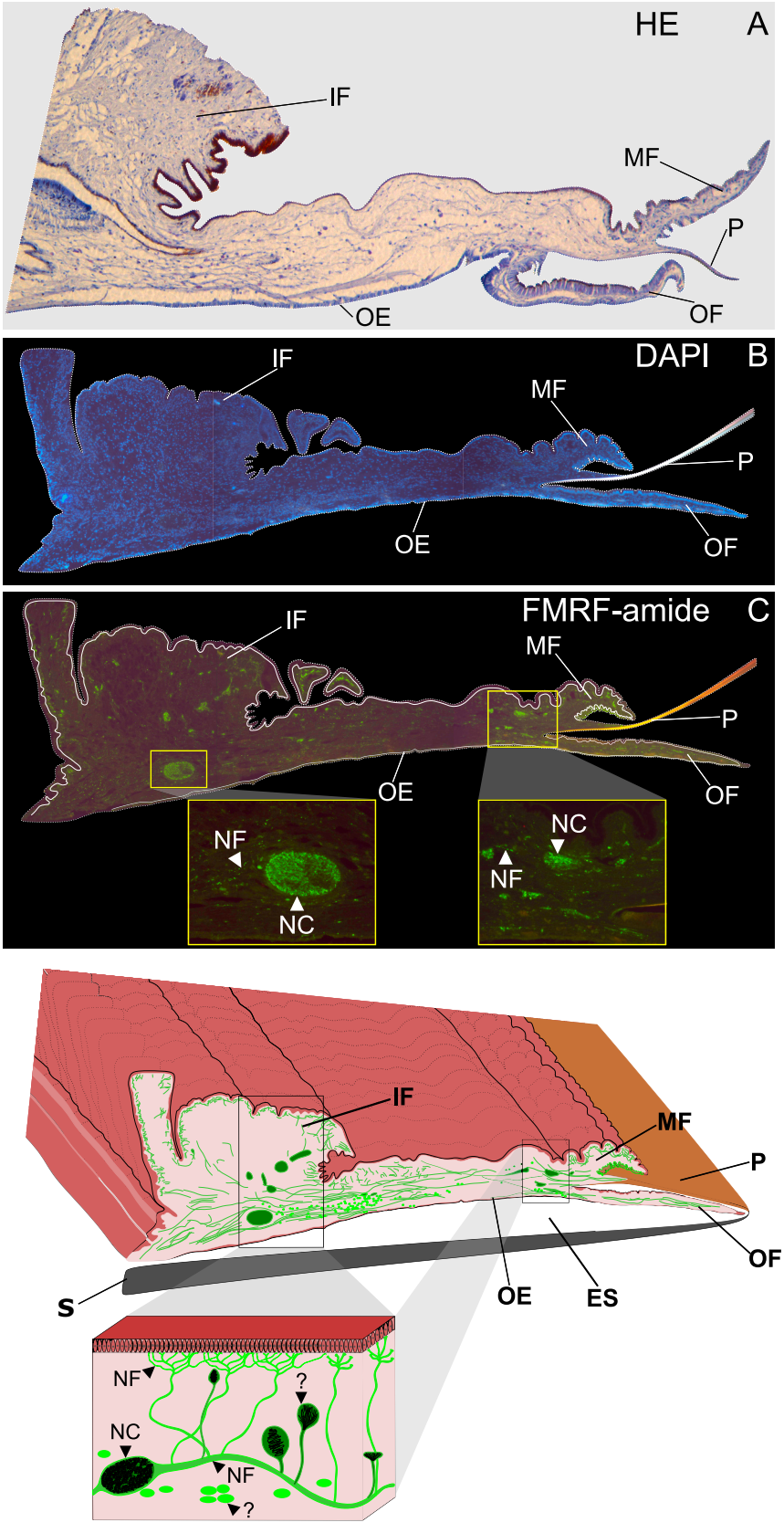

(caption on next page)

Fig. 2. Histology and immunohistochemistry of the *M. galloprovincialis* mantle. A) H&E staining of the mantle edge revealing the loosely packed mantle tissue in the three mantle folds and intensely staining epithelial cells particularly in the OE and OF. B) DAPI staining, C) immunostaining with the FMRF antibody, D) illustration of the distribution of the neuropeptide fibres in the mantle. The three structural folds of the mantle edge are represented. White arrows indicate the neural nodes within the mantle body. OF - outer fold; MF - middle fold; IF - inner fold, P - periostracum, OE- outer epithelial cell layer, NC - neuro cell clusters, NF-nerve fibres, S-shell, ES-extrapallial space. The scale is indicated in the images. Stained sections from histology were analysed using a microscope (Leica DM2000) connected to a digital camera (Leica DFC480) and the Immunohistochemistry sections were analysed using light or fluorescence microscopy and a Zeiss Axioimager Z2 (Carl Zeiss Group) coupled to a digital camera (Axiocam ICC3) linked to a computer for digital image analysis. The magnification used was 100× for the combined overall tissue images, and 200× for the detailed images.

CPG ganglion (CPG-group) and the left and right VG ganglion (VG-group) were severed, and shell regeneration was monitored in the drilled shell animals (Fig. 4 and Supplementary Fig. 5). Both the CPG and VG were independently severed since both nerve ganglia are suggested to control mantle function [14]. After severing the ganglia, the effect on shell regrowth was monitored using the approach outlined in Section 3.3.1. In *M. galloprovincialis*, regrowth of the shell was stopped in both the right and left valves when the CPG was severed during the experiments (Fig. 4A and B). In contrast, when the VG ganglia commissure was severed shell regrowth occurred as normal in both the left and right valves and the repair rate was identical to the control group after 7 days (Supplementary Fig. 5A and B). Visual inspection of the severed CPG or VG ganglia revealed that the nerve connections were not re-established for the duration of the experiment (data not shown). The results indicate that the CPG ganglia is essential for shell regrowth and may regulate the shell-related activities of the mantle. While the VG ganglia does not appear to have an important role.

To verify if the effects of the severed CPG on shell regrowth were due to modified mantle movement, mussels with a severed CPG were observed across the 20 days of the experiment. The results showed that cutting the commissure of the GPG or VG ganglia did not have any effect on mantle movement (Supplementary Fig. 5C).

3.3.3. CPG and VG ganglia reorganization after severing the ganglia or during shell damage

Immunohistochemistry was performed to analyse the impact of shell damage or cutting the commissure (CPG only) on neurons and nerve tracts in the CPG and VG ganglion and mantle at the initial stages of shell repair (24 h). Anti β-tubulin was used to analyse the overall nervous tissue organization and anti-5-HT to characterize the distribution of the neurotransmitter neurons/fibres (Fig. 5). In shell-damaged animals, the CPG ganglion showed a reorganized pattern. The immunopositive neurons for β-tubulin and 5-HT showed that the ganglion was re-organized compared to intact control animals (Fig. 5A). Twenty-four (24) hours after shell damage, the CPG ganglion in shell damaged animals was smaller than the control ganglion and contained a compact mass of 5-HT neurons. When the CPG commissure was severed (CPG-group) the shape of the ganglion changed, becoming rounder, and the 5-HT neurons became concentrated in the region localized near the severed commissure (Fig. 5A). For the VG-group, shell damage increased the ganglion size and 5-HT positive neurons became concentrated in the centre of the ganglion (Fig. 5B). Notably when the CPG commissure was severed the VG ganglion was affected and it became smaller, and the 5-HT neurons were concentrated on one side (Fig. 5B).

At the mantle edge, shell damage did not modify the tissue structure, but the distribution of the 5-HT positive fibres was modified. Shell damage increased the number of 5-HT positive fibres in the mantle but in the CPG-group there was a re-distribution of the 5-HT immunopositive nerves, and they became more concentrated in the mantle OF, which is most related with shell formation (Fig. 6).

3.3.4. Activity of biomineralization enzymes in the mantle

To determine the impact of shell damage and the nervous system on "shell toolbox genes" the activity of the biomineralization enzymes: α-carbonic anhydrase (CA) involved in the production of bicarbonate ions essential for crystal mineralization [71,72], acid phosphatase (TRAP) which is associated with shell remodelling and alkaline phosphatase (ALP) a shell matrix protein associated with shell formation [73,74] were measured in the mantle 10 days after shell drilling (Fig. 7A). In the SD-group the activity of CA and TRAP was significantly increased after shell damage ($p < 0.05$) compared to the intact group, but in the CPG-group shell damage caused a significant decrease in enzyme activities (Fig. 7A). This suggests that the activity of mantle cells producing the biomineralization enzymes is likely to be regulated by the nervous system. ALP activity did not change in any of the experimental groups (Fig. 7A).

3.3.5. Neuropeptide gene expression during shell regeneration

To identify potential candidates for shell repair, we selected 10 neuropeptide mantle transcripts for gene expression analysis in the mantle and CPG ganglia during the first 36 h after shell damage, which represents the initial stages of shell regeneration. Among these, the CALC precursors (CALCI and CALCII) were chosen due to their previously demonstrated potential involvement in shell production [46].

Expression data confirmed that all candidate precursors were expressed in both the mantle and CPG ganglia and that gene expression in both organs was modified after the shell was damaged (Fig. 7B, Supplementary Fig. 6). Expression of gene transcripts for APGW-amide, Myomodulin, LFRF-amide, FxRI-amide, LFRY-amide and LRNFV-amide peptide precursors was significantly increased in response to shell damage ($p < 0.05$) in both the mantle and CPG ganglia. In contrast, the AST-C gene was only significantly up-regulated in the mantle ($p < 0.05$). Shell damage did not invoke a significant change in gene expression of CALC (CALCI and CALCII) or the CCK/SK precursors either in the mantle or the CPG ganglia (Fig. 7B, Supplementary Fig. 6).

Candidate gene expression in later stages of shell repair was examined in the mantle 10 days after approximately 60 % of the drilled holes had been repaired (Fig. 3). The results showed that the pattern of gene expression was altered in both the SD-group and CPG-group (Fig. 7C). Six of the 10 candidate neuropeptide precursor genes had a coordinated expression pattern. In the SD-group transcript abundance of the CALCII, LFRY-amide, APWG-amide, Myomodulin, LFRF-amide and FxRI-amide peptide precursor genes was significantly increased ($p < 0.05$), but in the CPG-group expression of the same neuropeptide precursor genes was significantly down-regulated ($p < 0.05$). This indicates that the cells expressing these neuropeptide precursors may be regulated by the CPG ganglia. Conversely, no alterations in gene expression were detected for CALCI, LRNFV-amide and CCK/SK peptide precursors in the CPG-group (Fig. 7C). Expression of the AST-C precursor in the mantle was significantly increased ($p < 0.05$) in the SD-group and CPG-group suggesting that cells expressing this neuropeptide gene are not under the regulation of the CPG ganglia. Overall, the results indicate that regulation of mantle cells expressing the neuropeptide precursor genes targeted in this study may be regulated by the CPG ganglia. These neuropeptides may be involved in shell growth and repair.

3.4. Effect of neuropeptides on shell regeneration and shell microstructure

To identify the candidate peptides that might be directly involved in shell repair, the mature peptides were injected into the adductor muscle of CPG-group animals with damaged shells. The rationale behind this was that by directly adding the peptide, it should be possible to rescue the severed CPG ganglia phenotype, which caused arrested shell repair. The peptides that were tested included CALCIa, CALCIIa, MYOc and

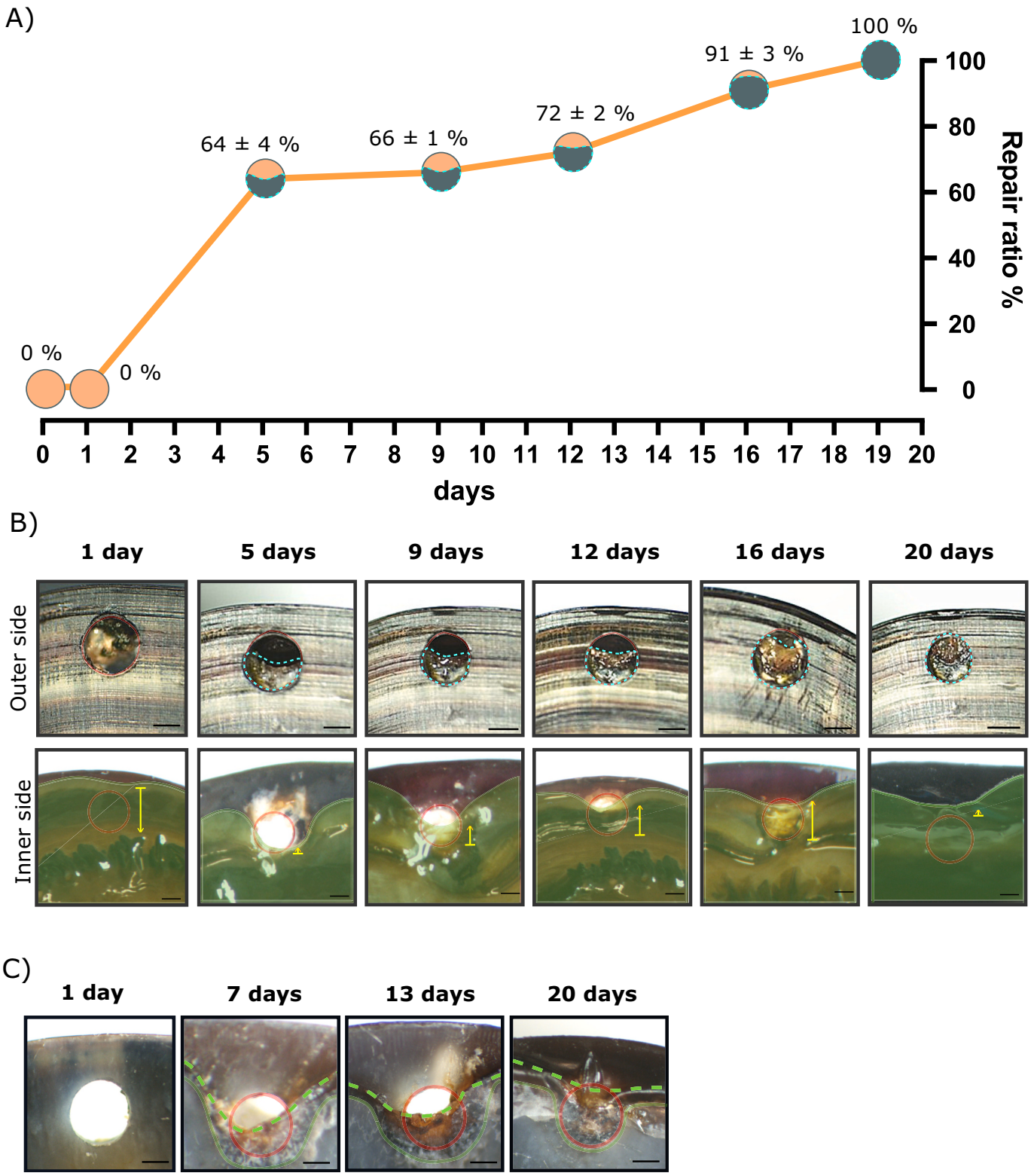

Fig. 3. Shell re-generation after damage in *M. galloprovincialis*. A)Timeline of the shell repair process. Images were analysed to calculate the percentage (%) shell repair ratio using Image J. The blue dashed line represents the outline of the newly grown shell. The orange line in the graph represents the progress of shell repair and the circles provide an illustrated view of the proportion (%) of the damaged shell that was repaired across time. The percentage presented is the average of the results of six different individuals. B) Digital images of the outer and inner shell side during shell repair. Outer shell side images illustrate hole coverage with the newly grown shell and inner shell side images illustrate the movement of the mantle during shell repair. The green shaded area represents the mantle, the red circles denote the edge of holes drilled in the shell, and the yellow arrows indicate the direction of mantle movement. C) Inner shell morphology during repair. The green line represents the baseline where the new shell begins to grow, the dashed green line represents the front of the newly deposited shell. The red circles indicate the hole position. The scale bar indicates 1 mm.

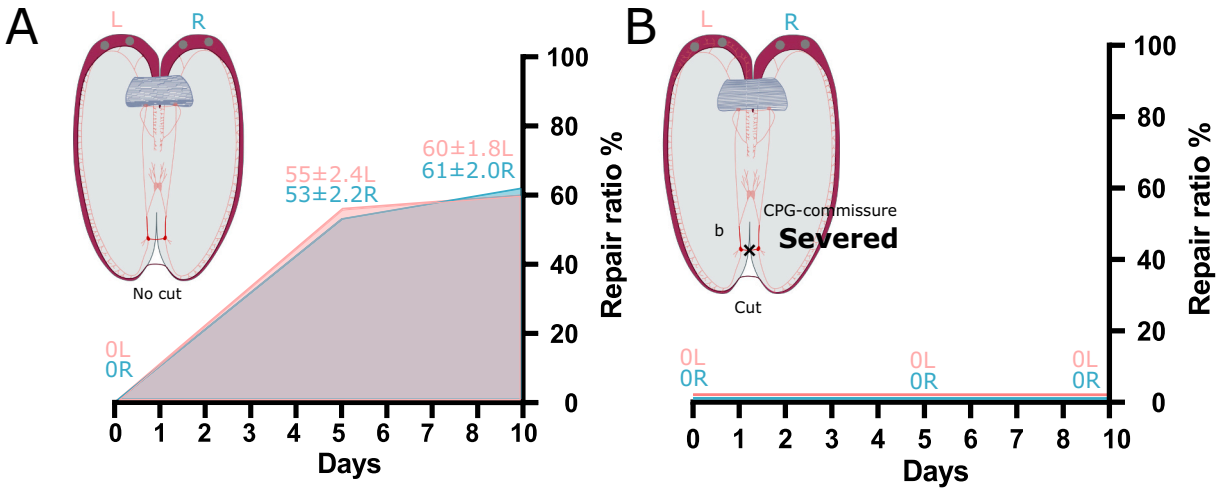

Fig. 4. Effect of ganglia commissure damage on shell regrowth. The nerve commissure that connects the CPG ganglia was severed and the process of shell-regrowth was observed for 10 days in both left and right valves. The repair of holes in the shell was monitored at 0, 5 and 10-days post-drilling, A) in animals ($n = 8$) in which holes were drilled in the shell (control-group) or B) in animals ($n = 8$) with drilled shells and severed ganglia (CPG-group). Two holes were made in each valve – the right valve is represented in blue; the left valve is represented in pink, using a stereomicroscope (Motic, SMZ-171, China) equipped with a digital camera (Visicam 6 Plus, VWR, Portugal). The percentage (%) of shell repair was calculated using Image J. No differences in the rate of shell repair were observed between the two valves. Shell repair was arrested in the animals in which the nerve commissure that connects the two CPGs was severed.

CCK/SK synthetic peptides. We chose CALCIa (encoded in the CALCI precursor) and CALCIIa (encoded in the CALCII precursor) because the precursors exhibited different gene expression profiles in response to shell damage (Fig. 7C). We selected the MYOc peptide (encoded in the Myomodulin precursor) because its gene expression was similar to that of the CALCII precursor (Fig. 7C). CCK/SK was used as a negative control since its gene expression was unrelated to shell repair (Fig. 7C). All peptides except for CCK significantly increased ($p < 0.05$) the rate of shell repair when compared to the drilled CPG-group animals where no peptide was supplied (Supplementary Fig. 7).

SEM photomicrographs of the inner side of the regenerated shells from the SD-group 15 days after drilling (when the hole was almost fully repaired, Supplementary Fig. 8A), showed that it was composed of tightly packed needle-like aragonite, mineralized calcium carbonate prismatic crystals (Fig. 8A). In the CPG-group that was injected with the CALCIa and CALCIIa mature peptides, SEM photomicrographs revealed the crystal structure of the newly grown shell was similar to the SD-group. The number of crystals formed in the newly regenerated shell in the CALCIa injected group was like the control and was higher than in the CALCIIa group where the crystals seemed to be sparser resulting in a porous-like structure in the regenerated shell (Supplementary Fig. 8B). Injections with the MYOc peptide promoted hole repair after 15 days (Supplementary Fig. 8A) but the microstructure did not contain typical biomineralized prismatic crystals and the regenerated shell was irregular and had spherical-like deposits that were mostly organic tissue (Fig. 8, Supplementary Fig. 8B).

The regenerated shell in all experimental groups was analysed by calcein staining and fluorescent microscopy. In the animals injected with CALCIa and CALCIIa peptides the regenerated shell had similar staining characteristics to the control group and revealed intense fluorescent staining corroborating the SEM photomicrographs (Fig. 8) and indicating the regenerated shell had a high content of $CaCO_3$ crystals (Supplementary Fig. 9). The fluorescence of the regenerated shell from animals injected with MYOc peptide was a scattered and diffuse suggesting that the material produced was poorly calcified and composed mainly of organic material (Supplementary Fig. 9). Heat-maps of the spectrum distribution obtained by ATR-FTIR in the regenerated shells supported the calcein staining results. The spectrum obtained in the regenerated shells of control animals and animals injected with CALCIa or CALCIIa peptide was very similar and was indicative of a high content and distribution of $CaCO_3$ (Supplementary Fig. 10). The ATR-FTIR results strongly supported the notion that the CALC peptides promoted the regeneration of shell with a $CaCO_3$ content and distribution characteristic of normal shell. The ATR-FTIR spectrum obtained for regenerated shell of animals treated with the MYOc peptide had a low content of $CaCO_3$ and it was primarily composed of organic matrix.

4. Discussion

Neuropeptides are signalling molecules and modulators of neuronal activity that regulate a diversity of physiological processes. Sequencing of bivalve nerve ganglia transcriptomes and genomes has identified a large variety of neuropeptide precursors, but their functions are poorly documented [23,61,75]. Neuropeptides that are homologues of those described in nerve ganglia of other bivalves were found in the mantle of *M. galloprovincialis* and associated with shell production and immunity [46–48,76]. Ganglia transcriptomes are not yet available for the mussel and the origin and potential regulation of the neuropeptide transcripts in the mantle remains elusive. Here we demonstrate that neuropeptides and the nervous system innervating the mantle seem to be key factors regulating the mantles function in shell production. The change in expression of neuropeptide genes in the mantle during shell repair or when it was impaired by damage to the CPG ganglia revealed an intriguing functional link between the CPG ganglia and the shell secretory activity of the mantle. Of note was the capacity of peptides of the CALC neuropeptides (CALCIa and CALCIIa) and MYOc to rescue shell repair when it was inhibited by cutting the commissure between the CPG ganglia. Several other putative neuropeptides responsive to shell drilling or CPG ganglia damage were identified as potential candidates for regulation of shell production by the mantle. Even though the neuroendocrine cells and putative neurosecretory cells responsible for neuropeptide expression in the mantle were not identified, in this study the evidence obtained indicates that neuropeptide gene expression in the mantle was responsive to shell status and most likely involves the nervous system.

4.1. *M. galloprovincialis* mantle innervation and regulation

The mantle is a multifunctional tissue involved in activities such as sensing, secretion, immunity, movement and feeding [77–80]. However,

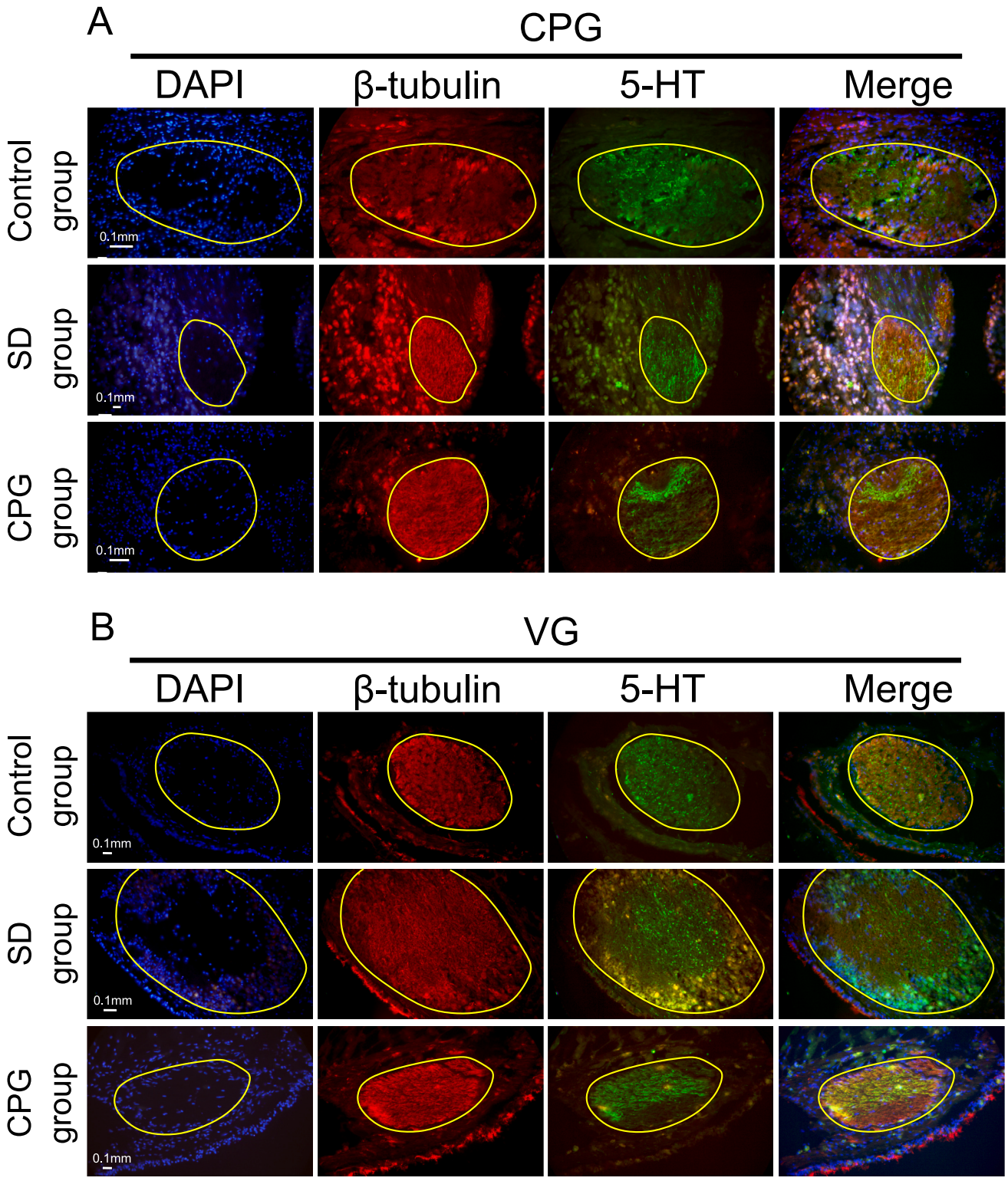

Fig. 5. Immunohistochemistry of *M. galloprovincialis* CPG and VG during shell regrowth. A) CPG ganglion, B) VG ganglion. The image shows immunostaining with DAPI and with anti-β-tubulin and anti-5-HT. SD-group- shell damage, CPG-group- shell damage with severed CPG ganglia after 24 h post damage. The scale bar is indicated. Stained sections were analysed using light or fluorescence microscopy and a Zeiss Axioimager Z2 (Carl Zeiss Group) coupled to a digital camera (Axiocam ICC3) linked to a computer for digital image analysis. The magnification used was 400×.

the best-known function of the mantle is the production of the biomineralized shell, and the most active region is the mantle edge [81,82]. The mantle edge is composed of three folds with heterogeneous function, the inner and middle folds have sensory and contractile activities, and the outer fold secretes the shell. The outer fold is contiguous with the outer mantle epithelium, and transports ions, matrix proteins, chitin and carbohydrates that create the shell scaffold and promote biomineralization of calcium carbonate [83–86]. Furthermore, mantle transcriptomes [45] revealed that the highly active mantle edge in *M. galloprovincialis* expressed a diversity of neuropeptide transcripts that

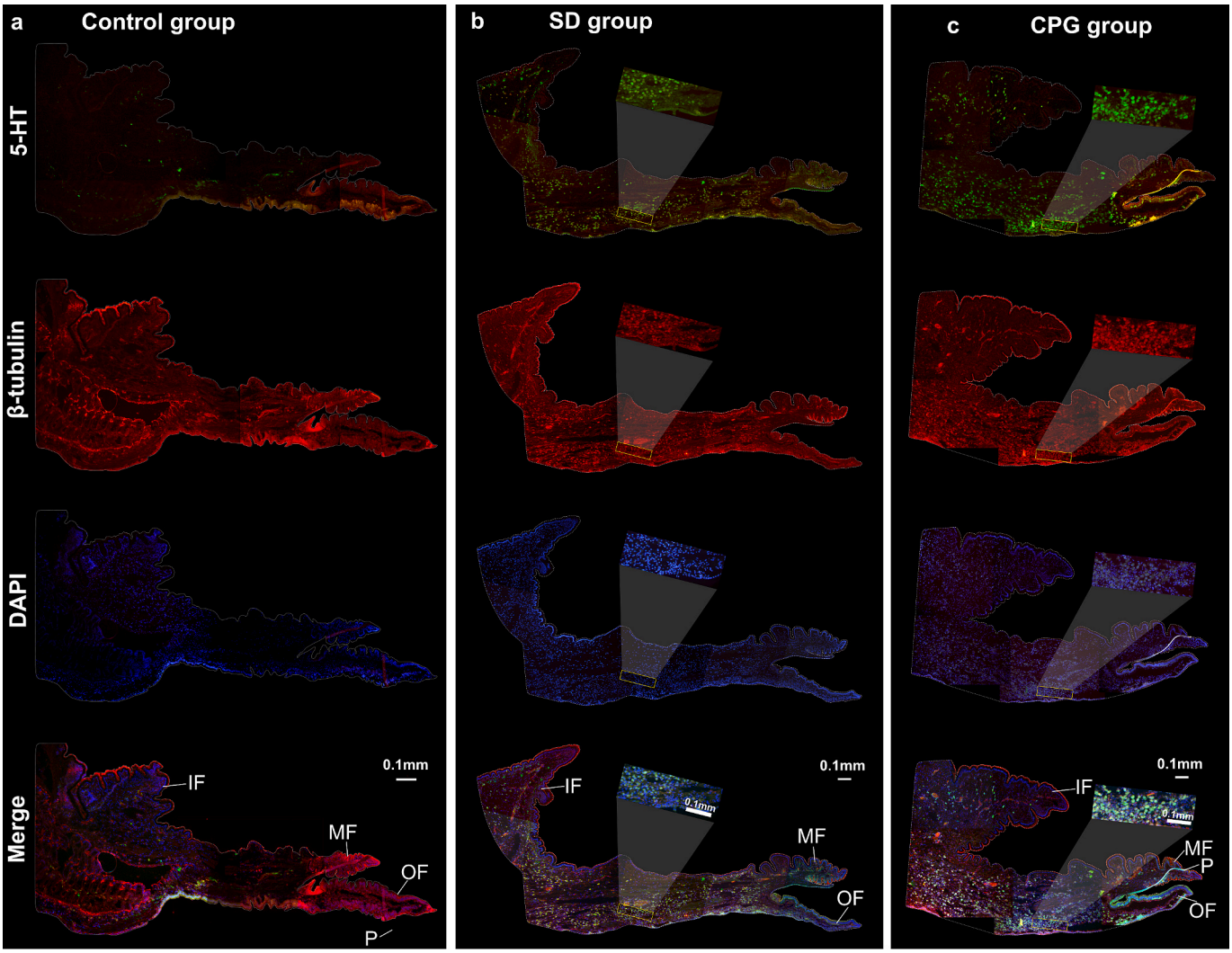

Fig. 6. Immunohistochemistry of the *M. galloprovincialis* mantle edge during shell regeneration. The image shows immunostaining with DAPI and with anti-β-tubulin and anti-5-HT of control, SD-group (shell damage) and CPG-group (shell damage with severed CPG ganglia) 24 h post damage. The scale bar is indicated and corresponds to 0.1 mm. The stained sections were analysed using light or fluorescence microscopy and a Zeiss Axioimager Z2 (Carl Zeiss Group) coupled to a digital camera (Axiocam ICC3) linked to a computer for digital image analysis. The magnification used was 200×.

were homologues of those in oyster (*M. gigas*) and scallop (*M. yessoensis*) ganglia [23,61]. Of the 48 neuropeptide gene families identified in the *M. galloprovincialis* genome only members of 3 gene families (Bursicon, GWE-amide and Neuropeptide prohormone 4) were not detected in mantle transcriptomes.

Although the nervous system in gastropods and cephalopods is relatively well characterized, it is much less studied in bivalves. In gastropods and cephalopods, the central nervous system (CNS) and the main components of their sensory system such as the eyes (optical lobes) and tentacles are localized in the head region. In gastropods seven pairs of ganglia, that regulate different organs are concentrated in the head region, and in the cephalopods which is the invertebrate with the most complex nervous system, they have large and well-developed brains divided into lobes [10]. In the bivalves a much simpler nervous system exists and is distributed throughout their body. Bivalves have no brain, and the nervous system consists of three pairs of symmetrical ganglia, the CPG, VG and PG, that project to, and innervate different parts of the body [55]. The CPG innervates the labial palps, anterior adductor muscle and the anterior mantle and sensory organs, the VG innervates the gills, heart, posterior adductor muscle, siphons, and posterior mantle [18,19,87–89] and the PG regulates the muscular foot, that is involved in locomotion and digging [6].

In the scallop (*P. yessoensis*), a bivalve, mapping by histochemistry of the nervous system revealed that the VG projects to and innervates the posterior region of the mantle margin [90]. Our immunofluorescence experiments revealed like in other bivalves the anterior and posterior mantle edge and inner mantle in *M. galloprovincialis* was highly innervated, particularly with FMRF an important biomarker of the nervous system in molluscs and other invertebrates [91–93] [85,94]. However, the results of the nerve sectioning experiment in the present study suggested that the CPG had a more pronounced role in regulating shell growth than the VG in *M. galloprovincialis*. Furthermore, the effect on shell growth of cutting the commissure of the CPG was not due to loss of mantle movement since the mantle crept forward and accompanied the repair of the drilled hole. Based on the results of the immunofluorescence with dense FMRF and 5-HT nerve clusters and the sectioning of the ganglia we propose a) that a mantle autonomous neurosecretory network exists and b) inputs from the CPG regulate shell secretion and repair.

4.2. A diversity of neuropeptide precursors in the mantle modulates shell production

Biomineralization is the biologically controlled process by which

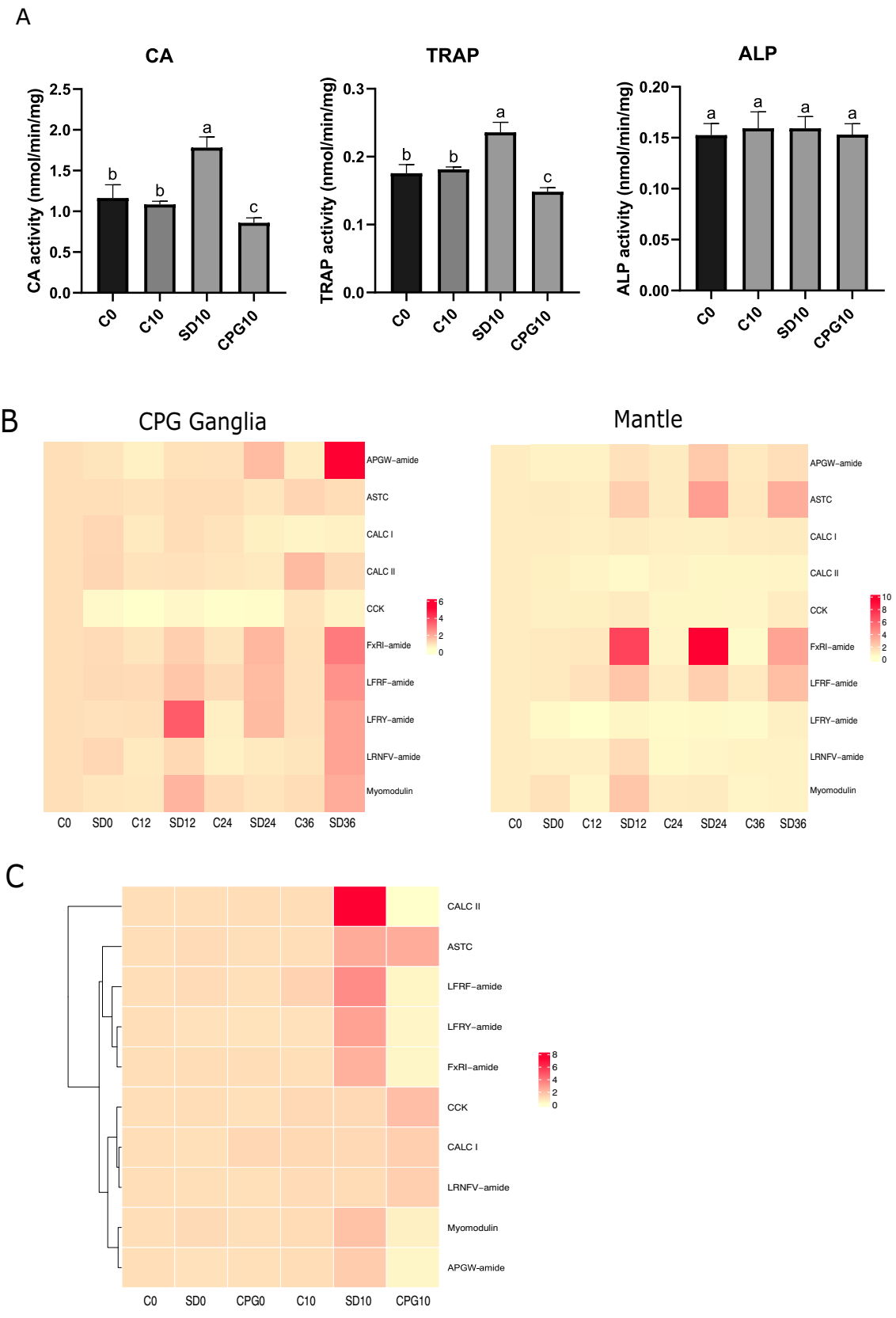

(caption on next page)

Fig. 7. Biomineralization enzyme activity and gene expression levels of candidate neuropeptides during shell re-generation. A) Enzyme activity of mantle edge samples (below the hole drilled in the shell) collected at day 0 and 10 days after repair. Three enzymes linked to biomineralization were measured: Alpha-Carbonic anhydrase (CA), Acid phosphatase (TRAP) and Alkaline phosphatase (ALP), in control (intact shell), drilled shells (SD-group) and drilled shells and ganglia damage (CPG-group) mussels. Values represent the mean ± SEM (n = 8/assay) performed in duplicate. Prism GraphPad v5 was used to assess the significance of the differences between the groups using One-Way Anova and Tukey's multiple comparison test. Different letters indicate significantly different groups ($p < 0.05$). B and C) Heat maps representing the clustering of gene expression profiles measured by qRT-PCR of the candidate neuropeptides, during early stages of shell repair in CPG ganglia and mantle (B) (Supplementary Fig. 6), and in late stages of shell repair in the mantle (C) (Supplementary Fig. 7). For B) mantle samples were collected from mussels with intact and drilled shells (SD-group) after 0, 12-, 24- and 36-hours. For C) mantle samples were collected from control (C), drilled shell (SD-group) and a drilled shell and severed ganglia (CPG-group) mussels at 0 and 10-day after shell damage. Hierarchical clustering of gene expression profiles is represented. In B) and C) gene expression levels were normalized using the geometric mean of two reference genes (EF1α and 18S). For B) ganglia results are shown as the mean of three samples/group (each sample contained the CPG from 2 individuals) and for the mantle represents the mean of six (n = 6) biological replicates per group/sampling point. For C) the results are shown as the mean of eight animals per group/sampling point. Heatmaps were prepared in R-studio software and the normalized values are represented using a colour gradient, from down-regulated (yellow) to up-regulated (red).

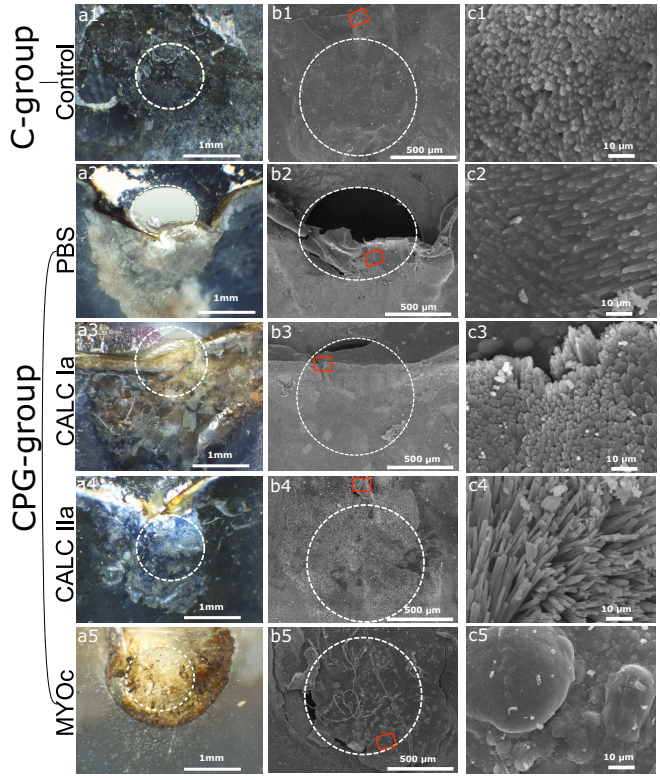

Fig. 8. Effect of neuropeptide injections on regrowing shell microstructure. Bright field (a) and SEM (b and c) digital images of the inner side of the right valve showing the recovery of the newly grown shell 15 days post-drilling. Bright field images were captured using a stereoscope (Motic, SMZ-171, China) equipped with a digital camera (Visicam 6 Plus, VWR, Portugal). The position of the drilled hole in (a) and (b) is indicated by a dashed circle and the red box. (b) reveals the microstructure of regrown shell analysed by SEM and (c) presents the same shell regrowth region but at a higher magnification. The numbers indicated in the images identifies the different groups: 1) non-injected control, and the CPG-severed group includes 4 different experimental groups: 2) PBS injected, 3) CALCIa injected, 4) CALCIIa injected and 5) MYOc injected. The control group represents the reference group and reveals the normal process of shell repair after damaging the shell by drilling.

living organisms generate mineralized structures [95]. The evolution of processes that regulate shell production has been associated with the diversity, expansion and success of the molluscs, and chitin has been implicated in this process [7–9]. In *M. galloprovincialis* with damaged shells the highest rates of shell growth regrowth occurred within the first 5 days of damage and >60 % of the hole in the shell valve was covered with biomineralized material. Using several different experimental approaches, we gathered evidence in the mussel that the ganglia is involved in the regulation of shell formation. Specifically, we identified neuropeptide precursors with a significantly modified gene expression from early stages of shell repair and these included APWG-amide, Myomodulin, LFRF-amide, FxRI-amide and LFRY-amide precursors that were previously described to regulate reproduction and growth in Mollusca [96–100]. The two mussel CALC peptide precursors we previously linked to shell biomineralization, CALCIa and CALCIIa [46], rescued the shell secretory ability of *M. galloprovincialis* mantle in individuals with a cut CPG commissure. Furthermore, the injection of CALCIa, and CALCIIa peptides promoted the formation of the tightly packed needle-like aragonite, mineralized calcium carbonate prismatic crystals characteristic of the nacreous layer [101]. In contrast, although MYOc promoted shell repair regular crystals were not formed, and an amorphous mass covered the hole. Further experiments will be required to better characterize the role in shell growth of the neuropeptides found in the bivalve mantle.

A large proportion of the predicted neuropeptide precursors (25 precursors out of 48) in the mantle encoded multiple mature peptides that based on their structure and the presence of conserved motifs are likely to be bioactive. Several of the candidate neuropeptide precursors tested to assess if they modify shell production encoded multiple mature peptides with different sequences and for which a function has not yet been assigned in *M. galloprovincialis*. Our results and those of other studies, namely the demonstration that oyster CALC activates oyster CALCRs *in vitro*, the presence of CALC peptides in the VG and the abundant repertoire of neuropeptide transcripts in bivalve mantle transcriptomes [49] support our hypothesis that peptides are regulatory factors of shell production.

4.3. Calcitonin is a key biomineralization regulatory factor in *M. galloprovincialis*

The involvement of the CALCII precursor, which encodes the peptide CALCIIa that was previously associated with calcium mobilization in the mussel mantle was confirmed [46], since it was highly up regulated in the mantle during shell repair, which suggests that it may act as a local regulator. Severing the commissure between the CPG ganglia caused a change in the expression of several candidate neuropeptide precursor genes in the mantle edge and biomineralization enzyme activity was inhibited. We showed that the administration of the neuropeptides CALCIa, CALCIIa and MYOc rescued the arrested shell repair phenotype and restored shell growth. However, although the shell growth stimulated by CALCIa and CALCIIa peptides had a similar morphological and structural appearance to the control (tightly packed calcium carbonate prismatic crystals), the regrown shell in the MYOc stimulated repair did not contain the characteristic prismatic crystals but rather was composed of irregular masses, which were revealed by calcein staining and ATR-FTIR analysis to have a low $CaCO_3$ content and to be mainly composed of organic matrix. In the mussels injected with CALC peptides shell regeneration was promoted and the new shell had a similar structure and composition to normal shell. We previously demonstrated that the CALC system can modify biomineralization enzymes and calcium movements in mantle epithelial cells [46] and in the present study we demonstrated an intact nervous connection with the ganglia is

required for shell secretion.

Neuropeptide receptors of the GPCR family, that shared conserved sequence and structure with the vertebrate and other invertebrate GPCRs, have been described in bivalves and other molluscs [76,102–104] but few have been functionally characterized. In bivalves CALCRs have been deorphanized in *M. gigas* and *M. galloprovincialis* and they are expressed in the mantle [46,49]. In *M. gigas* two CALC (Cragi-CT1b and Cragi-CT2b) orthologues of the mussel CALCIb and CALCIIb peptides (which we did not study) activated two cognate GPCRs (Cg-CT-R and Cragi-CTR2) in *M. gigas* [49]. However, the peptides Cragi-CT1a and Cragi-CT2dp, which are orthologues of the *M. galloprovincialis* peptides we studied (CALCIa and CALCIIa) did not activate these receptors, suggesting that CALC peptides that are encoded within the same precursor may have different biological roles. In *M. galloprovincialis* six CALCRs have been described and a receptor for the CALCIIa peptide was deorphanized and receptor gene expression shown to be sensitive to changes in salinity of the environmental water [46]. Receptors for AST-C [105,106], CCK [107–109], LFRF-amide peptides [110], myomodulin peptides [111] FxRI-amide [112] have been identified in Mollusca but few have been deorphanized and characterized in bivalves. In summary, neuropeptides are well represented in the mantle and nervous system of the mussel and most likely other bivalves and through their action *via* specific receptors in the mantle cells regulate shell production.

5. Conclusion

Shell production and biomineralization is a complex mechanism and its regulation is largely unknown. Here we provide functional evidence that neuropeptides play an important regulatory role in shell growth in bivalves. We found that in the bivalve *M. galloprovincialis* the mantle was a highly innervated organ with neuropeptide secreting fibres which are likely involved in shell production. Analysis of publicly available mantle transcriptomes revealed a high proportion of neuropeptides encoded in the genome of a diversity of bivalves were expressed and encoded for multiple mature peptides in the mantle of *M. galloprovincialis*. Furthermore, the gene expression of some neuropeptide precursors in the mantle changed during shell production and when the CPG commissure was severed suggesting these processes are linked. We identified a putative regulatory link between nerve ganglia and mantle neuropeptide gene expression and mantle biomineralization enzyme activity. In mussels with arrested shell growth caused by severing the CPG ganglia (but not the VG) the arrested phenotype could be rescued by injection of neuropeptides into the adductor muscle. The present results confirm previous studies proposing that the CALC peptide system is a key regulatory system in mussel shell growth since in mussels with a damaged shell, CALCIa and CALCIIa induced the formation of shell with a similar crystalline structure and composition to intact shells. The peptide, Myomodulin, contributed to repair of the damaged shell but the new shell had a low $CaCO_3$ content and instead of prismatic crystals an amorphous mass was produced. Overall, we provide strong evidence that neuropeptides and the nervous system regulate mantle function and shell growth in *M. galloprovincialis* and most likely other bivalves.

Abbreviations

CPG	Cerebropleural ganglia
CALC	Calcitonin
CNS	Central nervous system
MYO	Myomodulin
CCK/SK	Cholecystokinin/sulfakinin
CA	α-carbonic anhydrase
TRAP	Acid phosphatase
ALP	Alkaline phosphatase
SD-group	Shell drilling
CPG-group	Shell drilled, CPG ganglia sectioned
OF	Outer fold
q-PCR	Real-time PCR
ef1α	Elongation factor 1-alpha
18s	18S ribosomal subunit
SEM	Scanning electron microscopy

Funding

This study received Portuguese national funds from FCT - Foundation for Science and Technology through institutional projects UIDB/04326/2020 (DOI:10.54499/UIDB/04326/2020), UIDP/04326/2020 (DOI:10.54499/UIDP/04326/2020), and LA/P/0101/2020 (DOI:10.54499/LA/P/0101/2020), and from the operational programmes CRESC Algarve 2020 and COMPETE 2020 through projects EMBRC.PT ALG-01-0145-FEDER-022121 and BIODATA.PT ALG-01-0145-FEDER-022231 and from FCT-funded project FCT-AGAKHAN/541666287/2019 HealthyBi4Namibe project. ZL was supported by a PhD scholarship from the China Scholarship Council.

CRediT authorship contribution statement

Zhi Li: Writing – review & editing, Writing – original draft, Methodology, Formal analysis, Data curation. **Maoxiao Peng:** Writing – original draft, Methodology, Data curation. **Rute C. Félix:** Methodology, Data curation. **João C.R. Cardoso:** Writing – review & editing, Writing – original draft, Project administration, Conceptualization. **Deborah M. Power:** Writing – review & editing, Writing – original draft, Project administration, Conceptualization.

Declaration of competing interest

The authors declare that there is no conflict of interests.

Acknowledgments

The authors would like to thank to Dr. Telmo Nunes from the microscopy unit of the Faculdade de Ciências da Universidade de Lisboa for the shell SEM images. We thank Dr. José Paulo Silva from CCMAR for his expert assistance in the shell ATR-FTIR analysis.

Appendix A. Supplementary data

Supplementary data to this article can be found online at https://doi.org/10.1016/j.ijbiomac.2024.136500.

Data availability

The raw RNA-seq data generated in this study have been deposited in the NCBI SRA with the project PRJNA995578 in N°. SAMN36494222. The deduced complete sequences of the *M. galloprovincialis* neuropeptides are available in the supplementary materials.

References

[1] K.M. Kocot, J.T. Cannon, C. Todt, M.R. Citarella, A.B. Kohn, A. Meyer, S. R. Santos, C. Schander, L.L. Moroz, B. Lieb, Phylogenomics reveals deep molluscan relationships, Nature 477 (2011) 452–456.
[2] A. Wanninger, T. Wollesen, The evolution of molluscs, Biol. Rev. 94 (2019) 102–115.
[3] S.A. Smith, N.G. Wilson, F.E. Goetz, C. Feehery, S.C.S. Andrade, G.W. Rouse, G. Giribet, C.W. Dunn, Resolving the evolutionary relationships of molluscs with phylogenomic tools, Nature 480 (2011) 364–367.
[4] J. Vinther, The origins of molluscs, Palaeontology 58 (2015) 19–34.
[5] K.M. Kocot, A.J. Poustka, I. Stöger, K.M. Halanych, M. Schrödl, New data from Monoplacophora and a carefully-curated dataset resolve molluscan relationships, Sci. Rep. 10 (2020) 101.
[6] W.F. Ponder, D.R. Lindberg, J.M. Ponder, Biology and Evolution of the Mollusca vol. 1, CRC Press, 2019.
[7] I. Weiss, Species-specific shells: chitin synthases and cell mechanics in molluscs, Zeitschrift Für Kristallographie-Crystalline Materials 227 (2012) 723–738.

[8] I.M. Weiss, F. Lüke, N. Eichner, C. Guth, H. Clausen-Schaumann, On the function of chitin synthase extracellular domains in biomineralization, J. Struct. Biol. 183 (2013) 216–225.
[9] I.M. Weiss, V. Schönitzer, N. Eichner, M. Sumper, The chitin synthase involved in marine bivalve mollusk shell formation contains a myosin domain, FEBS Lett. 580 (2006) 1846–1852.
[10] B.U. Budelmann, The cephalopod nervous system: what evolution has made of the molluscan design, in: The Nervous Systems of Invertebrates: An Evolutionary and Comparative Approach: With a Coda Written by TH Bullock, Springer, 1995, pp. 115–138.
[11] I. Ellis, S.C. Kempf, Characterization of the central nervous system and various peripheral innervations during larval development of the oyster Crassostrea virginica, Invertebr. Biol. 130 (2011) 236–250.
[12] A.L. Hodgkin, A.F. Huxley, Action potentials recorded from inside a nerve fibre, Nature 144 (1939) 710–711.
[13] A.L. Hodgkin, A.F. Huxley, Resting and action potentials in single nerve fibres, J. Physiol. 104 (1945) 176.
[14] P.R. Benjamin, G. Kemenes, K. Staras, Molluscan nervous systems, in: Encyclopedia of Life Sciences, 2021, pp. 1–15, https://doi.org/10.1002/9780470015902.a0029277.
[15] V. Hartenstein, The central nervous system of invertebrates, in: The Wiley Handbook of Evolutionary Neuroscience, 2016, pp. 173–235.
[16] L. v Salvini-Plawen, Zur Morphologie und Phylogenie der Mollusken: die Beziehungen der Caudofoveata und der Solenogastres als Aculifera, als Mollusca und als Spiralia, Zeitschrift Fur Wissenschaftliche Zoologie 184 (1972) 205–394.
[17] G. Haszprunar, On the origin and evolution of major gastropod groups, with special reference to the Streptoneura, J. Moll. Stud. 54 (1988) 367–441.
[18] P.G. Beninger, M. Le Pennec, Structure and function in scallops, in: Developments in Aquaculture and Fisheries Science, Elsevier, 2006, pp. 123–227.
[19] E. Gosling, Marine Bivalve Molluscs, John Wiley & Sons, 2015.
[20] M. O'Shea, M. Schaffer, Neuropeptide function: the invertebrate contribution, Annu. Rev. Neurosci. 8 (1985) 171–198.
[21] V. Erspamer, A. Anastasi, Structure and pharmacological actions of eledoisin, the active endecapeptide of the posterior salivary glands of Eledone, Experientia 18 (1962) 58–59.
[22] A.L. De Oliveira, A. Calcino, A. Wanninger, Extensive conservation of the proneuropeptide and peptide prohormone complement in mollusks, Sci. Rep. 9 (2019) 4846.
[23] M. Zhang, Y. Wang, Y. Li, W. Li, R. Li, X. Xie, S. Wang, X. Hu, L. Zhang, Z. Bao, Identification and characterization of neuropeptides by transcriptome and proteome analyses in a bivalve mollusc Patinopecten yessoensis, Front. Genet. 9 (2018) 197.
[24] V. Van In, N. Ntalamagka, W. O'Connor, T. Wang, D. Powell, S.F. Cummins, A. Elizur, Reproductive neuropeptides that stimulate spawning in the Sydney Rock Oyster (Saccostrea glomerata), Peptides (N.Y.) 82 (2016) 109–119.
[25] M. de Jong-Brink, A. Ter Maat, C.P. Tensen, NPY in invertebrates: molecular answers to altered functions during evolution, Peptides (N.Y.) 22 (2001) 309–315.
[26] C. Zatylny-Gaudin, P. Favrel, Diversity of the RFamide peptide family in mollusks, Front. Endocrinol. (Lausanne) 5 (2014) 178.
[27] A.M. Abdraba, A.S.M. Saleuddin, Protein synthesis in vitro by mantle tissue of the land snail Otala lactea: possible insulin-like peptide function, Can. J. Zool. 78 (2000) 1527–1535.
[28] L. Gricourt, G. Bonnec, D. Boujard, M. Mathieu, K. Kellner, Insulin-like system and growth regulation in the Pacific oyster Crassostrea gigas: hrIGF-1 effect on protein synthesis of mantle edge cells and expression of an homologous insulin receptor-related receptor, Gen. Comp. Endocrinol. 134 (2003) 44–56.
[29] A.S.M. Saleuddin, V.M. Sevala, V.L. Sevala, S.T. Mukai, H.R. Khan, Involvement of mammalian insulin and insulin-like peptides in shell growth and shell regeneration in molluscs, Hard Tissue Mineralization Demineralization (1992) 149–169.
[30] R.M. Dillaman, A.S.M. Saleuddin, G.M. Jones, Neurosecretion and shell regeneration in Helisoma duryi (Mollusca: Pulmonata), Can. J. Zool. 54 (1976) 1771–1778.
[31] A.S.M. Saleuddin, S.C. Kunigelis, Neuroendocrine control mechanisms in shell formation, Am. Zool. 24 (1984) 911–916.
[32] W.P.M. Geraerts, Control of growth by the neurosecretory hormone of the light green cells in the freshwater snail Lymnaea stagnalis, Gen. Comp. Endocrinol. 29 (1976) 61–71.
[33] A.B. Smit, E. Vreugdenhil, R.H.M. Ebberink, W.P.M. Geraerts, J. Klootwijk, J. Joosse, Growth-controlling molluscan neurons produce the precursor of an insulin-related peptide, Nature 331 (1988) 535–538.
[34] J. Widjenes, N.W. Runham, Studies on the control of growth in Agriolimax reticulatus (Mollusca, Pulmonata), Gen. Comp. Endocrinol. 31 (1977) 154–156.
[35] J.D. Taylor, M. Layman, The mechanical properties of bivalve (Mollusca) shell structures, Palaeontology 15 (1972) 73–87.
[36] F. Marin, N. Le Roy, B. Marie, The formation and mineralization of mollusk shell, Front. Biosci.-Scholar 4 (2012) 1099–1125.
[37] V. Louis, L. Besseau, F. Lartaud, Step in time: biomineralisation of bivalve's shell, Front. Mar. Sci. 9 (2022) 906085.
[38] M. Suzuki, H. Nagasawa, Mollusk shell structures and their formation mechanism, Can. J. Zool. 91 (2013) 349–366.
[39] M.S. Clark, M.A.S. Thorne, F.A. Vieira, J.C.R. Cardoso, D.M. Power, L.S. Peck, Insights into shell deposition in the Antarctic bivalve Laternula elliptica: gene discovery in the mantle transcriptome using 454 pyrosequencing, BMC Genomics 11 (2010) 1–14.
[40] M.G. Alves, P.F. Oliveira, Effects of non-steroidal estrogen diethylstilbestrol on pH and ion transport in the mantle epithelium of a bivalve Anodonta cygnea, Ecotoxicol. Environ. Saf. 97 (2013) 230–235.
[41] N.A. Bjärnmark, T. Yarra, A.M. Churcher, R.C. Felix, M.S. Clark, D.M. Power, Transcriptomics provides insight into Mytilus galloprovincialis (Mollusca: Bivalvia) mantle function and its role in biomineralisation, Mar. Genomics 27 (2016) 37–45.
[42] A. Carini, T. Koudelka, A. Tholey, E. Appel, S.N. Gorb, F. Melzner, K. Ramesh, Proteomic investigation of the blue mussel larval shell organic matrix, J. Struct. Biol. 208 (2019) 107385.
[43] T. Yarra, K. Gharbi, M. Blaxter, L.S. Peck, M.S. Clark, Characterization of the mantle transcriptome in bivalves: Pecten maximus, Mytilus edulis and Crassostrea gigas, Mar. Genomics 27 (2016) 9–15.
[44] T. Yarra, M. Blaxter, M.S. Clark, A bivalve biomineralization toolbox, Mol. Biol. Evol. 38 (2021) 4043–4055.
[45] M. Peng, C.R.J. Cardoso, G. Pearson, V.M.A. Canário, M.D. Power, Core genes of biomineralization and cis-regulatory long non-coding RNA regulate shell growth in bivalves, J. Adv. Res. 64 (2023) 117–129.
[46] J.C.R. Cardoso, R.C. Félix, V. Ferreira, M. Peng, X. Zhang, D.M. Power, The calcitonin-like system is an ancient regulatory system of biomineralization, Sci. Rep. 10 (2020) 1–18.
[47] Z. Li, J.C.R. Cardoso, M. Peng, J.P.S. Inácio, D.M. Power, Evolution and potential function in molluscs of neuropeptide and receptor homologues of the insect allatostatins, Front. Endocrinol. (Lausanne) 12 (2021) 725022.
[48] J.C.R. Cardoso, R.C. Félix, N. Bjärnmark, D.M. Power, Allatostatin-type A, kisspeptin and galanin GPCRs and putative ligands as candidate regulatory factors of mantle function, Mar. Genomics 27 (2016) 25–35.
[49] J. Schwartz, E. Réalis-Doyelle, M.-P. Dubos, B. Lefranc, J. Leprince, P. Favrel, Characterization of an evolutionarily conserved calcitonin signalling system in a lophotrochozoan, the Pacific oyster (Crassostrea gigas), J. Exp. Biol. 222 (2019) jeb201319.
[50] Y. Kuroki, T. Kanda, I. Kubota, T. Ikeda, Y. Fujisawa, H. Minakata, Y. Muneoka, FMRFamide-related peptides isolated from the prosobranch mollusc Fusinus ferrugineus, Acta Biol. Hung. 44 (1993) 41–44.
[51] D.A. Price, M.J. Greenberg, Structure of a molluscan cardioexcitatory neuropeptide, Science 197 (1977) (1979) 670–671.
[52] V. Lopez, L. Wickham, L.U.C. Desgroseillers, Molecular cloning of myomodulin cDNA, a neuropeptide precursor gene expressed in neuron L10 of Aplysia californica, DNA Cell Biol. 12 (1993) 53–61.
[53] E. Kellett, S.J. Perry, N. Santama, B.M. Worster, P.R. Benjamin, J.F. Burke, Myomodulin gene of Lymnaea: structure, expression, and analysis of neuropeptides, J. Neurosci. 16 (1996) 4949–4957.
[54] Y. Kuroki, T. Kanda, I. Kubota, Y. Fujisawa, T. Ikeda, A. Miura, Y. Minamitake, Y. Muneoka, A molluscan neuropeptide related to the crustacean hormone, RPCH, Biochem. Biophys. Res. Commun. 167 (1990) 273–279.
[55] E. Kotsyuba, A. Kalachev, P. Kameneva, V. Dyachuk, Distribution of molecules related to neurotransmission in the nervous system of the mussel Crenomytilus grayanus, Front. Neuroanat. 14 (2020) 35.
[56] K.J. Adamson, T. Wang, M. Zhao, F. Bell, A.V. Kuballa, K.B. Storey, S.F. Cummins, Molecular insights into land snail neuropeptides through transcriptome and comparative gene analysis, BMC Genomics 16 (2015) 1–15.
[57] S. Andrews, FastQC: A Quality Control Tool for High Throughput Sequence Data. https://www.bioinformatics.babraham.ac.uk/projects/fastqc/, 2010.
[58] A.M. Bolger, M. Lohse, B. Usadel, Trimmomatic: a flexible trimmer for Illumina sequence data, Bioinformatics 30 (2014) 2114–2120.
[59] M. Peng, C.R.J. Cardoso, P. Sorigué, M.D. Power, Species-specific Responses of Bivalves to Ocean Acidification, (Unpublish), 2024.
[60] M.J. Stewart, P. Favrel, B.A. Rotgans, T. Wang, M. Zhao, M. Sohail, W. A. O'Connor, A. Elizur, J. Henry, S.F. Cummins, Neuropeptides encoded by the genomes of the Akoya pearl oyster Pinctata fucata and Pacific oyster Crassostrea gigas: a bioinformatic and peptidomic survey, BMC Genomics 15 (2014) 1–16.
[61] E. Réalis-Doyelle, J. Schwartz, C. Cabau, L. Le Franc, B. Bernay, G. Rivière, C. Klopp, P. Favrel, Transcriptome profiling of the Pacific oyster Crassostrea gigas visceral ganglia over a reproduction cycle identifies novel regulatory peptides, Mar. Drugs 19 (2021) 452.
[62] M. Gerdol, R. Moreira, F. Cruz, J. Gómez-Garrido, A. Vlasova, U. Rosani, P. Venier, M.A. Naranjo-Ortiz, M. Murgarella, S. Greco, Massive gene presence-absence variation shapes an open pan-genome in the Mediterranean mussel, Genome Biol. 21 (2020) 1–21.
[63] F. Madeira, M. Pearce, A.R.N. Tivey, P. Basutkar, J. Lee, O. Edbali, N. Madhusoodanan, A. Kolesnikov, R. Lopez, Search and sequence analysis tools services from EMBL-EBI in 2022, Nucleic Acids Res. 50 (2022) W276–W279.
[64] O.V. Yurchenko, V.A. Dyachuk, Characterization of Neurodevelopment in Larvae of the Protobranch Acila insignis (Gould, 1861) in order to reconstruct the last common ancestor of bivalves, Malacologia 64 (2022) 241–255.
[65] V.E. Nikishchenko, E.M. Sayenko, V.A. Dyachuk, First immunodetection of sensory and nervous systems of parasitic larvae (glochidia) of freshwater bivalve Nodularia douglasiae, Front. Physiol. 13 (2022) 624.
[66] C. Rodriguez-Navarro, Ö. Cizer, K. Kudłacz, A. Ibañez-Velasco, C. Ruiz-Agudo, K. Elert, A. Burgos-Cara, E. Ruiz-Agudo, The multiple roles of carbonic anhydrase in calcium carbonate mineralization, CrystEngComm 21 (2019) 7407–7423.
[67] W.E.G. Müller, H.C. Schröder, U. Schlossmacher, M. Neufurth, W. Geurtsen, M. Korzhev, X. Wang, The enzyme carbonic anhydrase as an integral component of biogenic Ca-carbonate formation in sponge spicules, FEBS Open Bio 3 (2013) 357–362.

[68] J.C.R. Cardoso, V. Ferreira, X. Zhang, L. Anjos, R.C. Félix, F.M. Batista, D. M. Power, Evolution and diversity of alpha-carbonic anhydrases in the mantle of the Mediterranean mussel (Mytilus galloprovincialis), Sci. Rep. 9 (2019) 10400.
[69] S. Pilecki, J. Katarzyna, The Importance of Fourier-Transform Infrared Spectroscopy in the Identification of Carbonate Phases Differentiated in Magnesium Content, 2019, pp. 32–42.
[70] B.H. Solis, Y. Cui, X. Weng, J. Seifert, S. Schauermann, J. Sauer, H.J. Freund, Initial stages of CO 2 adsorption on CaO: a combined experimental and computational study, Phys. Chem. Chem. Phys. 19 (6) (2017) 4231–4242.
[71] B.C. Tripp, K. Smith, J.G. Ferry, Carbonic anhydrase: new insights for an ancient enzyme* 210, J. Biol. Chem. 276 (2001) 48615–48618.
[72] S. Lindskog, J.E. Coleman, The catalytic mechanism of carbonic anhydrase, Proc. Natl. Acad. Sci. 70 (1973) 2505–2508.
[73] N. Le Roy, D.J. Jackson, B. Marie, P. Ramos-Silva, F. Marin, The evolution of metazoan α-carbonic anhydrases and their roles in calcium carbonate biomineralization, Front. Zool. 11 (2014) 1–16.
[74] N. Le Roy, D.J. Jackson, B. Marie, P. Ramos-Silva, F. Marin, Carbonic anhydrase and metazoan biocalcification: a focus on molluscs, in: Key Eng Mater, Trans Tech Publ, 2016, pp. 151–157.
[75] M.A. Kim, K. Markkandan, N.-Y. Han, J.-M. Park, J.S. Lee, H. Lee, Y.C. Sohn, Neural ganglia transcriptome and peptidome associated with sexual maturation in female Pacific abalone (Haliotis discus hannai), Genes (Basel) 10 (2019) 268.
[76] J.C.R. Cardoso, J.C. Mc Shane, Z. Li, M. Peng, D.M. Power, Revisiting the evolution of family B1 GPCRs and ligands: insights from mollusca, Mol. Cell. Endocrinol. 112192 (2024).
[77] P.G. Beninger, A. Veniot, Y. Poussart, Principles of pseudofeces rejection on the bivalve mantle: integration in particle processing, Mar. Ecol. Prog. Ser. 178 (1999) 259–269.
[78] B. Allam, E.P. Espinosa, Bivalve immunity and response to infections: are we looking at the right place? Fish Shellfish Immunol. 53 (2016) 4–12.
[79] R. Windoffer, A. Jahn, F. Meyberg, J. Krieger, O. Giere, Sulphide-induced metal precipitation in the mantle edge of *Macoma balthica* (Bivalvia, Tellinidae)–a means of detoxification, Mar. Ecol. Prog. Ser. 187 (1999) 159–170.
[80] B. Morton, Feeding and digestion in Bivalvia, the Mollusca, Physiology Part 2 (1983) 65–147.
[81] C.M. Yonge, Mantle fusion in the Lamellibranchia, Pubblicazioni Della Stazione Zoologica Di Napoli 29 (1957) 151–171.
[82] C.M. Yonge, Symmetries and the role of the mantle margins in the bivalve Mollusca, Malacol. Rev. 16 (1983) 1–10.
[83] C.A. Richardson, N.W. Runham, D.J. Crisp, A histological and ultrastructural study of the cells of the mantle edge of a marine bivalve, Cerastoderma edule, Tissue Cell 13 (1981) 715–730.
[84] L. Addadi, S. Weiner, Control and design principles in biological mineralization, Angew. Chem. Int. Ed. Engl. 31 (1992) 153–169.
[85] J.A. Audino, J.E.A.R. Marian, A. Wanninger, S.G.B.C. Lopes, Mantle margin morphogenesis in Nodipecten nodosus (Mollusca: Bivalvia): new insights into the development and the roles of bivalve pallial folds, BMC Dev. Biol. 15 (2015) 1–22.
[86] B. Morton, M. Peharda, The biology and functional morphology of Arca noae (Bivalvia: Arcidae) from the Adriatic Sea, Croatia, with a discussion on the evolution of the bivalve mantle margin, Acta Zool. 89 (2008) 19–28.
[87] W.S. Bullough, Practical Invertebrate Anatomy, 1958.
[88] P.S. Galtsoff, The American Oyster, *Crassostrea virginica* gmelin, US Government Printing Office, 1964.
[89] H. Grizel, An atlas of histology and cytology of marine bivalve molluscs, in: An Atlas of Histology and Cytology of Marine Bivalve Molluscs, 2003.
[90] T. Matsutani, T. Nomura, Localization of monoamines in the central nervous system and gonad of the scallop Patinopecten yessoensis, Bull. Jpn. Soc. Sci. Fish. 50 (1984) 425–430.
[91] G.A. Cottrell, The wide range of actions of the FMRFamide-related peptides and the biological importance of peptidergic messengers, Comp. Mol. Neurobiol. (1993) 279–285.
[92] N. Santama, P.R. Benjamin, Gene expression and function of FMRFamide-related neuropeptides in the snail Lymnaea, Microsc. Res. Tech. 49 (2000) 547–556.
[93] C. Zatylny-Gaudin, P. Favrel, Diversity of the RFamide peptide family in mollusks, Front. Endocrinol. (Lausanne) 5 (2014) 110140.
[94] A.S.M. Saleuddin, R.M. Dillaman, Direct innervation of the mantle edge gland by neurosecretory axons in helisoma duryi (Mollusca: Pulmonata), Cell Tissue Res. 171 (1976) 397–401.
[95] A.S.M. Saleuddin, K.M. Wilbur, The Mollusca: Physiology, Part 2, Academic Press, 2012.
[96] B. Bernay, M. Baudy-Floc'h, B. Zanuttini, C. Zatylny, S. Pouvreau, J. Henry, Ovarian and sperm regulatory peptides regulate ovulation in the oyster Crassostrea gigas, Mol. Reprod. Dev. Inc. Gamete Res. 73 (2006) 607–616.
[97] R.P.J. De Lange, J. Joosse, J. Van Minnen, Multi-messenger innervation of the male sexual system of Lymnaea stagnalis, J Comp Neurol 390 (1998) 564–577.
[98] J.M. Koene, Neuro-endocrine control of reproduction in hermaphroditic freshwater snails: mechanisms and evolution, Front. Behav. Neurosci. 4 (2010) 167.
[99] R.M. Hoek, K.W. Li, J. Van Minnen, J.C. Lodder, M. de Jong-Brink, A.B. Smit, R. E. Van Kesteren, LFRFamides: a novel family of parasitation-induced-RFamide neuropeptides that inhibit the activity of neuroendocrine cells in Lymnaea stagnalis, J. Neurochem. 92 (2005) 1073–1080.
[100] F. Morishita, Y. Furukawa, O. Matsushima, H. Minakata, Regulatory actions of neuropeptides and peptide hormones on the reproduction of molluscs, Can. J. Zool. 88 (2010) 825–845.
[101] I. Kobayashi, T. Samata, Bivalve shell structure and organic matrix, Mater. Sci. Eng. C 26 (2006) 692–698.
[102] O. Mirabeau, J.-S. Joly, Molecular evolution of peptidergic signaling systems in bilaterians, Proc. Natl. Acad. Sci. 110 (2013) E2028–E2037.
[103] G. Jékely, Global view of the evolution and diversity of metazoan neuropeptide signaling, Proc. Natl. Acad. Sci. 110 (2013) 8702–8707.
[104] M.R. Elphick, O. Mirabeau, D. Larhammar, Evolution of neuropeptide signalling systems, J. Exp. Biol. 221 (2018) jeb151092.
[105] M.M. Díaz, M. Schlichting, K.C. Abruzzi, X. Long, M. Rosbash, Allatostatin-C/AstC-R2 is a novel pathway to modulate the circadian activity pattern in Drosophila, Curr. Biol. 29 (2019) 13–22.
[106] H.-M. Jiang, Z. Yang, Y.-Y. Xue, H.-Y. Wang, S.-Q. Guo, J.-P. Xu, Y.-D. Li, P. Fu, X.-Y. Ding, K. Yu, Identification of an allatostatin C signaling system in mollusc Aplysia, Sci. Rep. 12 (2022) 1213.
[107] N. Yu, G. Smagghe, CCK (−like) and receptors: structure and phylogeny in a comparative perspective, Gen. Comp. Endocrinol. 209 (2014) 74–81.
[108] T. Janssen, E. Meelkop, M. Lindemans, K. Verstraelen, S.J. Husson, L. Temmerman, R.J. Nachman, L. Schoofs, Discovery of a cholecystokinin-gastrin-like signaling system in nematodes, Endocrinology 149 (2008) 2826–2839.
[109] J. Schwartz, M.-P. Dubos, J. Pasquier, C. Zatylny-Gaudin, P. Favrel, Emergence of a cholecystokinin/sulfakinin signalling system in Lophotrochozoa, Sci. Rep. 8 (2018) 16424.
[110] S. Yoon, M.A. Kim, J.S. Lee, Y.C. Sohn, Functional analysis of LFRFamide signaling in Pacific abalone, *Haliotis discus hannai*, PLoS One 17 (2022) e0267039.
[111] L. Bigot, I. Beets, M.-P. Dubos, P. Boudry, L. Schoofs, P. Favrel, Functional characterization of a short neuropeptide F-related receptor in a lophotrochozoan, the mollusk Crassostrea gigas, J. Exp. Biol. 217 (2014) 2974–2982.
[112] S.M. Pedder, Y. Muneoka, R.J. Walker, Structure–activity and possible mode of action of S-Iamide neuropeptides on identified central neurons of Helix aspersa, Regul. Pept. 101 (2001) 131–140.
[113] I.A. Field, Biology and Economic Value of the Sea Mussel Mytilus Edulis, US Government Printing Office, 1922.